Stony Brook University

Developing Tools for Cavin-1 Purification and Binding Studies with Caveolin-1

A Thesis Presented

by

Safa Farjand Siddiqui

to

The Graduate School

in Partial Fulfillment of the

Requirements

for the Degree of

Master of Science

in

Biochemistry and Cell Biology

Stony Brook University

August 2015

Stony Brook University

The Graduate School

Safa Farjand Siddiqui

We, the thesis committee for the above candidate for the

Master of Science degree, hereby recommend

acceptance of this thesis.

Deborah Brown, PhD
Department of Biochemistry and Cell Biology

Jarrod French, PhD
Department of Chemistry

This thesis is accepted by the Graduate School

Charles Taber
Dean of the Graduate School

Abstract of the Thesis

Developing Tools for Cavin-1 Purification and Binding Studies with Caveolin-1

by

Safa Farjand Siddiqui

Master of Science

in

Biochemistry and Cell Biology

Stony Brook University

2015

Caveolae are nanoscale invaginations found in the plasma membrane of mammalian cells, and are implicated in numerous essential cellular communication and transport processes. They are characterized by a coat composed of caveolin and cavin proteins. Recent studies of the caveolar coat complex suggest that cavin-1 associates with caveolin-1 during caveolae biogenesis. However, it is not known how this binding occurs. Studies of the spatial and physical interactions between cavin-1 and caveolin-1 can provide valuable insights into the mechanism of caveolae generation. The goal of this study was to test two different fusion tags to purify a sufficient quantity of cavin-1, for use in future binding studies with caveolin-1. We successfully generated a plasmid encoding 6His-SUMO-cavin-1 by cloning full length cavin-1 into the LIC SUMO vector 2S-T, and expressed it in BL21 (DE3) pLysS. Parameters of temperature, concentration of IPTG, detergent type, and length of incubation after IPTG-induction, were tested to optimize cavin-1 expression conditions. Immobilized metal affinity chromatography with Ni-NTA resin tested binding and release of the SUMO-tagged cavin-1. The poor protein yields from tests on 6-His-SUMO-cavin-1 underscored persistent issues of solubility, suboptimal binding to the resin, and inadequate release of purified protein. Studies on an earlier construct, GST-cavin-1, were then resumed to evaluate and maximize binding and release of GST-cavin-1 from glutathione-agarose beads. While inefficient bead binding

problems remained, GST-cavin-1 yielded a more consistent recovery of the desired protein. As results suggested that enough soluble GST-cavin-1 could be obtained for binding studies, we performed a large-scale preparation of the protein for use in a diagnostic test for association with caveolin-1. We did not observe any binding in this preliminary test. The results prompted further questions about the stoichiometry of the cavin-1 and caveolin-1 complex, and highlighted the possibility of additional layers of complexity involved in this interaction.

Table of Contents

List of Figures

List of Abbreviations

BME: β-mercaptoethanol
CAV1: caveolin-1
CAV2: caveolin-2
CAV3: caveolin-3
CCVs: clathrin-coated vesicles
CMC: critical micelle concentration
DRM: detergent resistant membranes
EB: elution buffer
EDTA: ethylenediaminetetraacetic acid
EM: electron microscopy
ER: endoplasmic reticulum
FRET: Förster resonance energy transfer
GST: glutathione S-transferase
HEK-293: human embryonic kidney-293
His: Histidine
HR1 : helical region 1
HSWB: high salt wash buffer
IMAC: immobilized metal affinity chromatography
IPTG: Isopropyl β-D-1-thiogalactopyranoside
kDa: kilodalton
MEF: murine embryonic fibroblasts
miniSOG: mini singlet oxygen generator
MMP13: matrix metalloproteinase-13
MURC: muscle related coil-coil protein
NTA: nitrilotriacetic acid
PBS: phosphate buffered saline
PIP: phosphatidylinositol phosphate
PKC: protein kinase C
PM: plasma membrane
PRKCDBP: protein kinase C delta binding protein
PS: phosphatidylserine
PTRF: polymerase transcript release factor
PVDF: polyvinylidene fluoride
SDPR: serum deprivation response protein
SDS-SB: sodium dodecyl sulfate-sample buffer
SDS-PAGE: sodium dodecyl sulfate- polyacrylamide gel electrophoresis
SUMO: small ubiquitin-like modifier
WB: wash buffer

Acknowledgments

I would like to thank my advisor, Dr. Brown, for giving me the rewarding opportunity to be a part of her lab, for introducing me to the cavin-1 purification project, and for teaching me many essential principles of research design. Working in her lab has been a highlight of my Stony Brook experience. I am truly grateful for all her guidance, inspiration and support.

I would like to thank Anne Ostermeyer-Fay for helping me grasp important concepts and techniques in the lab. It was an honor working with her this year.

I would like to thank Dr. French for his advice, valuable feedback and suggestions while writing this thesis.

I would like to thank the Biochemistry and Cell Biology Department at Stony Brook and Professor Neta Dean for letting me be a part of this program and welcoming community. I have made many wonderful friends at Stony Brook.

I would also like to express my sincere gratitude to my parents, who have provided me with unconditional love, support and encouragement throughout my endeavors.

Chapter 1

INTRODUCTION

1.1 The Landscape of the Plasma Membrane and Caveolae

The plasma membrane (PM) is a dynamically structured mosaic characterized by non-randomly distributed hierarchically built supramolecular protein complexes, distinct membrane subdomains with specialized functions created by localized lipids and protein assemblies, and mobile biomolecules in a viscous phospholipid bilayer (Krijnse Locker and Schmid, 2013; Vereb et al., 2003). Liquid-ordered and –disordered states can coexist on the PM (Razani et al., 2002). Its fluid architecture facilitates the continuous restructuring and rearrangement of macromolecular membrane clusters in response to cellular requirements and environmental stimuli (Vereb et al., 2003). The PM is the site of signaling and trafficking events implicated in many vital important cellular communication, transport and metabolic processes. A salient feature of the eukaryotic PM is the specialized compartmentalization of the surface into domains of distinct function.

Caveolae are specialized internalizing structures and remarkable examples of the complex organization of the eukaryotic PM. They are characteristic and morphological nanoscale 60-80 nm wide ampullate invaginations present abundantly on the PM of many mammalian cells (Hill et al., 2008). Though often described as flask-shaped, they are more crater-like in appearance, with a less constricted neck at the opening (Hill et al., 2008). Initially recognized as exclusively smooth membrane invaginations, the description of caveolae has expanded to accommodate other morphologies (Razani et al., 2002). Grape-like clusters, fused elongated tubules and *trans*-cellular channels are nontraditional structures of caveolae and are usually tissue-specific (Razani et al., 2002). With more strides in research, caveolae can no longer be considered static structures in the PM, but rather dynamic features capable of conglomeration and fusion events leading to various disparate morphologies (Razani et al., 2002).

While not as well-characterized as another internalizing membrane structure, the clathrin-coated vesicle (CCV), many facets of caveolae function and composition have been revealed.

Caveolae are pleiotropic in nature and are involved in a host of critical cellular processes such as signaling, endothelial transcytosis, lipid homeostasis, mechanosensation, and mitigation of mechanical stress (Hansen and Nichols, 2010; Kovtun et al., 2014; Parton and del Pozo, 2013; Razani et al., 2002). They can serve as functional scaffolds, creating microenvironments to regulate signaling efficiency and outcome through cross talk between different signal transduction pathways (Krijnse Locker and Schmid, 2013; Razani et al., 2002). Caveolar trafficking at the PM is important for the endocytosis of some viruses, such as human papillomavirus. Caveolae can be found in most mammalian cell types, with varying levels of abundance according to tissue specificity. Vertebrate adipocytes, endothelial cells, type I pneumocytes, fibroblasts and smooth muscle cells contain high concentrations of caveolae (Palade and Predescu, 1953; Napolitano, 1963; Mobley and Eisenberg, 1975; Gabella, 1976; Gil, 1983; Razani et al., 2002), while central nervous system neurons and lymphocytes are devoid of these membrane invaginations (Fra et al., 1994; Cameron et al., 1997). The density of caveolae within individual cells may also vary; the basolateral surface of epithelial cells and the rear of migrating cells can have higher concentrations of caveolae (Parton and del Pozo, 2013), while the Golgi does not contain morphological caveolae (Hansen and Nichols, 2010; Mogelsvang et al., 2004). Caveolar dysfunction has been linked to several human health problems, such as "lipodystrophy, muscular dystrophies, osteoporosis, cardiovascular disorders and cancers" (Parton and del Pozo, 2013).

1.2 The Caveolin Family

Liquid ordered domains, present in a cholesterol-dependent state in which lipids exhibit extended acyl chains and pack tightly together, can form through the coalescence of cholesterol and sphingolipids (Brown and London, 1998; Razani et al., 2002; Simons and Toomre, 2000). These can be termed "lipid rafts". Caveolae microdomains share many of the biochemical properties of lipid rafts (Razani et al., 2002). The detergent resistance and buoyancy of these microdomains make them conducive to purification techniques such as sucrose gradient ultracentrifugation (Lisanti et al., 1994; Razani et al., 2002). However, the purification of caveolae has been more difficult than that of CCVs, requiring detergents and

sonication steps which may compromise the quality of purified products through the loss of components or possible contamination (Krijnse Locker and Schmid, 2013). Thus, the identification and understanding of coat components driving caveolae formation has lagged behind that of CCVs (Krijnse Locker and Schmid, 2013). Studies over the years have gradually paved a better understanding of the molecular characterization of caveolae.

The hallmark discovery of caveolin as a key structural constituent of the caveolar coat resulted from a serendipitous convergence of disparate interests (Krijnse Locker and Schmid, 2013; Razani et al., 2002; Rothberg et al., 1992). In an antibody screen for tyrosine-phosphorylated substrates of Rous sarcoma virus-transformed fibroblasts, Glenney and Zokas identified caveolin as a predominant substrate (Glenney and Zokas, 1989; Razani et al., 2002). Antibodies to this 22 kDa protein showed nonrandom, punctate staining along the plasma membrane in a manner similar to that of caveolae craters (Glenney and Zokas, 1989; Rothberg et al., 1992). Rothberg and colleagues used immunogold EM to demonstrate the nearly complete localization of caveolin to caveolae (Razani et al., 2002; Rothberg et al., 1992).

Caveolins are multiply acylated integral membrane proteins with a single, long, hydrophobic cholesterol-binding domain (Hansen and Nichols, 2010; Kovtun et al., 2014; Kurzchalia et al., 1992; Monier, 1995, Rothberg et al., 1992). They are embedded in the cytosolic leaflet of the cell membrane, with a central hydrophobic domain present as a hairpin loop, with amino- and carboxy-terminal domains present in the cystol (Hansen and Nichols, 2010; Kovtun et al., 2014; Kurzchalia et al., 1992; Monier, 1995, Rothberg et al., 1992). Caveolins are inserted into the membrane of the endoplasmic reticulum and travel through the secretory pathway. They form high molecular weight homo-and heteroligomers in the Golgi apparatus and are transported to the PM as poorly-characterized assemblies of 100-200 caveolin molecules (Hansen and Nichols, 2010; Monier, 1995; Parton and del Pozo, 2013; Pelkmans and Zerial, 2005; Tagawa et al., 2005). Caveolin oligomerization is thought to promote caveolae formation by driving PM curvature and inward invagination (Krijnse Locker and Schmid, 2013). A synergistic relationship may exist between the oligomeric meshwork and cholesterol to elicit membrane bending and distortion (Razani et al., 2002).

The mammalian caveolin family contains three isoforms of the protein, encoded by three distinct genes. Expression of the caveolin isoforms is tissue-specific. Caveolin-1 (CAV1) is the major caveolin isoform and is essential for caveolae formation in non-muscle cells (Ludwig et al., 2013). It forms a highly ordered, detergent-resistant complex of 14-16 monomeric units and cotranslationally enters membranes via the ER translocation apparatus (Monier, 1995; Razani et al., 2002). Expression of CAV1 in cells lacking the protein induces caveolae formation. Caveolin-2 (CAV2) is similarly distributed, and forms stable hetero-oligomers with CAV1 (Sowa, 2011), though its expression is not crucial for forming caveolae. Striated muscle cells require the expression of the muscle-specific caveolin-3 (CAV3) to drive the formation of these membrane invaginations (Park et al, 2002).

Mutations or the absence of caveolins are linked to many detrimental disorders. Phenotypes of caveolin knockouts include adipose tissue abnormalities, muscle myopathies, compromised angiogenesis, disruption of the nitric oxide signaling pathway, and altered susceptibility to conditions such as atherosclerosis, and tumorigenesis (Hansen and Nichols, 2010; Le Lay and Kurzchalia, 2005). For example, CAV1 knockout mice can have altered endothelial permeability, lipid dysregulation, and insulin resistance, while deficiencies in CAV3 may lead to muscle conditions known as caveolinopathies (Ludwig et al., 2013; Parton and Del Pozo, 2013).

1.3 The Cavin Protein Family

Until recently studies of caveolar machinery had primarily focused on caveolins. Although caveolins are essential for caveolae biogenesis, accessory proteins and kinases have been reported to modulate levels of regulation and function, challenging the previous notion of caveolae as stable domains (Bastiani et al., 2009). The physical and spatial assembly of these complex coat proteins during caveolae formation has been an elusive question. New insights have been gained on a second family of soluble caveolin binding partners, the cavins. Cavin proteins are cytosolic caveolar coat protein components that are indispensable in the biogenesis of morphologically identifiable caveolae, in influencing their dynamics, and in

forming stable protein arrays involved in membrane remodeling (using their coincident PIP and PS binding sites) (Kovtun et al., 2014; Krijnse Locker and Schmid, 2013).

The four different mammalian isoforms of cavins are encoded by four distinct genes, and exhibit more heterogeneity among the family than do the caveolins. The four cavins were all previously identified in other contexts and given distinct names, before their similarities were recognized. Cavin-1 is polymerase transcript release factor (PTRF), cavin-2 is serum deprivation protein response (SDPR), cavin 3 is protein kinase C, delta binding protein (PRKCDBP/SRBC) and cavin-4 is muscle-related coiled-coil protein (MURC) (Bastiani et al., 2009; Ludwig et al., 2013). The cavin proteins have high sequence homology in the N-terminal region and tissue specific expression profiles. They represent a single protein family, sharing a similar primary structure characterized by a conserved N-terminal domain containing "heptad repeats of hydrophobic residues" and a basic adjacent region (Hansen and Nichols, 2010). The hydrophobic residues impart a propensity to form coiled coils. Cavins 1-3 are predicted to have a putative leucine zipper region which forms a triple-helix coiled-coil (Bastiani et al., 2009; Kovtun et al., 2014), and the polybasic regions of cavin-1 suggest their utility as nuclear localization signals (Bastiani et al., 2009). Cavins are often post-translationally modified, which may be a possible explanation for their SDS-PAGE migration at molecular weights 10-15 kDa greater than that predicted from their primary structure (Hansen and Nichols, 2010; Vinten et al., 2005). The phosphorylation of cavins may play a role in the budding of caveolae from the plasma membrane. Caveolins 1-2, and cavins 1-3 exhibit similar tyrosine phosphorylation profiles during insulin signaling (Hansen and Nichols, 2010). Like that of caveolins, deficiencies of cavins exhibit detrimental phenotypes, such as cardiomyopathies, muscle disorders and problems with lipid metabolism (Gambin et al., 2014; Parton and Del Pozo, 2013).

Cavin-1/PTRF is a peripheral membrane protein ubiquitously expressed in all cells that contain caveolin and is essential for morphologically recognizable caveolae formation *in vivo* (Krijnse Locker and Schmid, 2013; Ludwig et al., 2013). Cavin-1 is expressed in both muscle and non-muscle tissues in an expression profile broader than that of CAV1 and CAV3 (Hansen and Nichols, 2010). The phenotypes of CAV1 and CAV3 double knockout mice are similar to those

lacking cavin-1, underscoring the central role of the latter in caveolar biogenesis and homeostasis (Hansen and Nichols, 2010; Park et al., 2002). PTRF was initially discovered in a yeast two-hybrid screen by Jansa and colleagues (1998) using transcription-termination factor (TTF)-I as the bait (Jansa et al., 1998; Hansen and Nichols, 2010), and identified as a nuclear protein *trans* factor capable of releasing paused ternary transcription complexes (Jansa et al., 1998; Gambin et al., 2014). The classification of cavin-1 as a prominent caveolar coat protein, in addition to a contributor to ribosomal RNA synthesis, was proposed by Vinten and colleagues (2005), who reported a positive correlation between cavin-1 and caveolin-1 concentrations and the presence of caveolae (Hansen and Nichols, 2010; Vinten et al., 2005).

Hill and colleagues (2008) identified PTRF in a comparative proteomic screen for putative caveolar proteins, using detergent resistant membranes (DRM) prepared from WT mouse fibroblasts and Cav1-/- murine embryonic fibroblasts (MEFs) (Hill et al., 2008). Western blotting showed that the immunoreactive band at 60 kDa for PTRF was significantly reduced in the caveolin knockout DRM. PTRF expression notably declined in Cav1 -/- adult mouse tissues as well, suggesting a functional association between PTRF and caveolin. However, no linkage between cavin and non-caveolar caveolin (from the Golgi, or mutant forms of caveolin) has been reported (Hill et al., 2008). Fluorescence resonance energy transfer studies (FRET) suggest that cavin-1 only associates with caveolin in nanometer proximity once both classes of molecules localize to the cell surface (Chadda and Mayor, 2008). This association is dependent on cholesterol availability; cholesterol depletion may disrupt the morphology of caveolae (Chadda and Mayor, 2008). The absence of cavin-PTRF expression in prostate cancer PC3 cells and during zebrafish notochord development correlated with a lack of caveolae (Hill et al., 2008). Inducing cavin-PTRF expression in PC3 triggers caveolae formation (Hill et al., 2008). Hill and colleagues (2008) proposed a model for caveolae biogenesis in which Cavin-PTRF is sequestered to membrane domains containing phosphatidylserine (PS), and cholesterol, while caveolin oligomers stabilize PM curvature. Cavin-1 helps transition caveolin oligomers from a flat profile to a more curved shape (Hansen and Nichols, 2010), thus producing the characteristic ampullate shape of caveolae (Hill et al., 2008). PTRF may regulate levels of caveolar and non-caveolar caveolin (Chadda and Mayor, 2008). PTRF-Cavin knockdown cells

release caveolins into the PM. These caveolins have decreased lateral mobility, reduced oligomeric size, and are rapidly degraded in lysosomes (Hill et al., 2008). The carefully modulated ratio of caveolar and non-caveolar caveolins is important for signaling outcomes and the turnover of caveolar coat constituents (Chadda and Mayor, 2008). The restriction of cavin-1 and caveolin-1 interactions to the plasma membrane suggests PTRF's role in transitioning the flat profile of caveolin-1 oligomers to the characteristic morphology of caveolae , a process that drives curvature and inward invagination of the membrane (Krijnse Locker and Schmid, 2013; Hansen and Nichols, 2010; Chadda and Mayor, 2008). Figure 1 on the following page illustrates a possible model of cavin-1 dependent caveolae formation.

Cavins 2-4 are more cell and tissue specific, with cavin-4 exclusively cardiac and skeletal muscle restricted (Gambin et al., 2014; Ludwig et al., 2013). These cavins were not originally discovered in association with the caveolae coat. Cavin-2 was first isolated from human platelets by Burgener and colleagues (1990). It was identified as a phosphatidylserine (PS)-binding protein and an *in vitro* substrate of protein kinase C (PKC) isoforms (Burgener et al., 1990; Hansen and Nichols, 2010). Greater cavin-2 expression is induced upon serum starvation. Similarly, cavin-3 was identified as a PS binding partner and PKC substrate. While the functions of cavins 2-4 are not as thoroughly studied, the role of cavin-2 in generating PM curvature has been suggested, while cavin-3 was found to affect the formation of caveolar endocytic vesicles (Parton and Del Pozo, 2013).

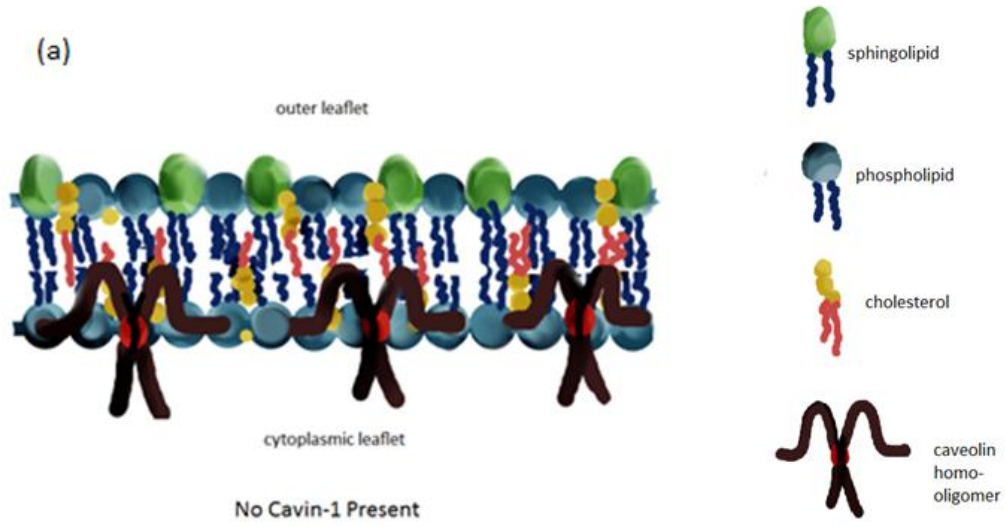

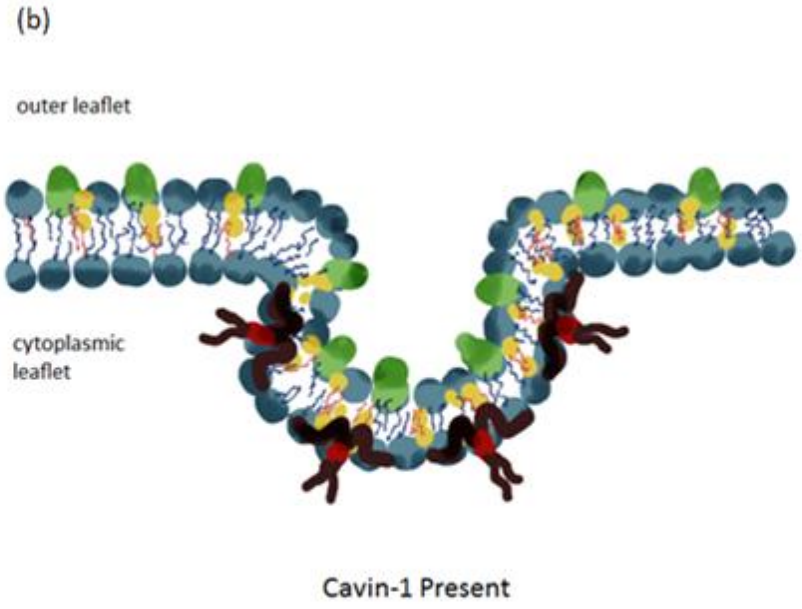

Figure 1: Possible Model of Caveolae Formation. a) When there is no cavin-1 present, caveolin-1 homo-oligomers are present at the PM. The PM has a flat profile. b) In the presence of cavin-1, caveolin-1 homo-oligomers interact with the PM to produce the characteristic curvature of caveolae. Image adapted from Razani et al., 2002.

1.4 Insights on Stoichiometry and Structure

Cavins exist as large, detergent-resistant complexes that are detectable on sucrose gradients, with sedimentation coefficients of 40S-60S (Hansen and Nichols, 2010; Ludwig et al., 2013) and can be co-immunoprecipitated with each other (Ludwig et al., 2013). The dynamics, spatial interactions and conformations involved in their associations with caveolins and within cavin complexes still require elucidation. Studies of this co-localization have been challenging, as cavins and caveolins do not co-fractionate on sucrose gradients of detergent-solubilized cell lysates (Ludwig et al., 2013). The association between caveolae and cavin was not readily made, as previous cavin purification attempts had led to dissociation from the caveolae coat (Krijnse Locker and Schmid, 2013). This hindered determination of the composition and stoichiometry of coat constituents.

Ludwig and colleagues (2013) used membrane cross-linking agents to stabilize associations among caveolar coat constituents. The stoichiometry of coat proteins was determined after isolation via detergent solubilization by sucrose gradient centrifugation and/or immunoisolation (Krijnse Locker and Schmid, 2013; Ludwig et al., 2013). The basic caveolar coat oligomer consists of trimeric cavin-1 bound to approximately 12 molecules of caveolin and one molecule of cavin-2 or -3 (Krijnse Locker and Schmid, 2013; Ludwig et al., 2013). The latter cavins compete as cavin-1 binding partners. There are between 140-150 core assembly units of caveolin molecules per caveolae, 10 of which are required for coat formation (Krijnse Locker and Schmid, 2013; Ludwig et al., 2013). The organization and biogenesis of the caveolae coat resembles that of the “basket-woven” clathrin coat of CCVs described by Brodsky and colleagues (2001), in which an outer shell composed of a clathrin triskelion interacts with an inner shell of clathrin-binding adaptor proteins (Brodsky et al., 2001; Krijnse Locker and Schmid, 2013; Ludwig et al., 2013). Ludwig and colleagues also fused the clonable tag, mini singlet oxygen generator (miniSOG), to either of the cavin isoforms to confirm their localization to the caveolar bulb, and not to the neck (Ludwig et al., 2013; Krijnse Locker and Schmid, 2013).

Gambin and colleagues (2014) developed a single-molecule fluorescence approach to study the self-assembly and stoichiometries among cavin protein complexes from purified cell lysates and *in vitro* synthesized components. They were able to demonstrate that two distinct

subcomplexes form among the cavins 1-3 from the complex interplay of unique homo- and hetero-oligomerization properties of each member, and their responses to changes in membrane stretch. While all three cavins can reside in the same caveolae, flattening of the membrane invagination due to changes in tension can trigger the release of coat components in discrete subcomplexes of 9(+/-2) cavin 1-cavin 2 and cavin 1-cavin 3 (Gambin et al., 2014). The homo-oligomerization of cavin 1 to cavins 2 and 3 occurs in a ratio between 2 and 3:1 (Gambin et al., 2014; Kovtun et al., 2014; Ludwig et al., 2013). Gambin et al (2014) suggested that pre-homo- and hetero-oligomerized cavin complexes may interact to form striated nanodomains around caveolae in a fashion that contrasts with clathrin coat assembly of CCVs (Gambin et al., 2014).

Kovtun and colleagues (2014) demonstrated that the universal oligomerization domain of cavins, helical region 1 (HR1), was necessary to promote their homo- and hetero-oligomerization. A structurally conserved trimeric coiled coil was reported, in which one molecule of either cavin 2 or 3 may be accommodated within the heterotrimeric coiled coil (Kovtun et al., 2014). The distinct packing geometry of the *a* and *d* positions of the cavin family heptad repeats and the possibility of surface-associated salt-bridge formation may explain this exclusion principle (Kovtun et al., 2014). The basic surface patch of the HR1 domain was proposed to interact with polyphosphoinositides and membrane binding sites in the cavin C terminus. This may anchor cavins to the PM and facilitate their role in membrane remodeling (Kovtun et al., 2014).

Despite the significant strides made in recent years regarding the composition of the caveolae coat, considerable gaps still remain in the literature. Further studies correlating the dynamics and interactions of caveolae in different tissues or cell lines with cavin complex formation need to be conducted (Hansen and Nichols, 2010). Additional functional characterization of cavin subcomplexes may provide more molecular explanations for the roles of caveolae. The mechanism by which caveolins and cavins associate to form the characteristic bulb-like invaginations remains unexplored (Kovtun et al., 2014). The oligomerization of caveolins, cavin-caveolin protein-protein interactions and cholesterol availability may

contribute to the ability of caveolins to form caveolae (Kovtun et al., 2014) but further investigation will provide much-needed insight.

1.5 Fusion Tags as Valuable Tools for Protein Studies

Much work has been invested in the discovery, advancement and refinement of techniques to optimize protein production. The development of genetically engineered fusion tags has been hailed as a hallmark achievement in improving the expression, solubility, proper protein folding and functional recovery of many recombinant proteins, particularly those difficult to express. Soluble recombinant protein is necessary in biochemical studies of structure and function. The selection, design and use of a fusion tag must be done with careful consideration regarding tag retention, and the possibility of extraneous sequences in the purified product (Chelur et al., 2008). Changes in protein conformation, compromised biological activity and toxicity of the target protein have been reported. Tag cleavage with a protease can be performed as a safeguard. However, the protease must also be judiciously selected.

1.5.1 The 6 X His Tag as an Affinity Tag of Choice

Affinity tags (e.g. polyhistidine affinity tag, or antibody-antigen) are widely used short peptide sequences fused to recombinant proteins. They are commonly using in various research areas, such as in high throughput expression studies for the functional characterization of new proteins. Affinity tags determine the genetic design of the fusion protein of interest (Arnau et al., 2006). The highly specific interactions involved between a ligand, either bound to a solid support or containing an immobilized antibody-detectable epitope, (Chelur et al., 2008) and the compound of interest can be exploited for selective binding to the stationary phase, resulting in a high degree of purification. Release of the protein molecules of interest from an affinity column can be done with an eluent to alter pH, ionic strength, or isoelectric point. Using a molecule that competes for a binding site is one of the most commonly used techniques to release the protein, such as the use of imidazole in Ni-IMAC.

The His-tag is the most commonly used affinity tag, utilizing principles of transition metal and coordination chemistry. Short His-tags are placed at either the N- or C-terminus of the

desired recombinant protein. Histidine's aromatic imidazole side chain has a high affinity for metal ion matrices. In immobilized metal affinity chromatography (IMAC), chelated metal ion ligands form a coordination complex with an immobilized chelating agent (Arnau et al., 2006). For example, in Ni-NTA affinity chromatography, the nitrilotriacetic acid (NTA) ligand occupies 4 of the 6 binding sites of the nickel ion. The two remaining sites can bind to the 6xHis-tag on the remaining protein of interest. When the cell-free crude extract from the host cell (often a bacteria) is poured through an affinity column, all other peptides without the tag will be eluted out, resulting in single-step protein purification in relatively high yield and purity.

1.5.2 Solubility Enhancing Tags: The SUMO Tag

Solubility-enhancing tags are large peptides or proteins that are fused to the protein of interest, and help promote proper folding in their binding partner to increase solubility of the recombinant protein (Eposito and Chatterjee, 2006). Ubiquitin-based tags, such as SUMO (small ubiquitin-like modifier), can be used as a viable alternative for increasing expression, production and solubility of otherwise intractable proteins or under-expressed proteins in *E. coli* (Arnau et al., 2006; Malakhov et al., 2004). The SUMO tag has been a valuable tool in purification, studies of protein-protein interaction, and small molecular drug discovery. SUMO's external hydrophilic surface and inner hydrophobic core may produce detergent-like effects, allowing previously insoluble proteins to fold properly and solubilize (Butt et al., 2005). Its flexible N- and C-termini maintain the integrity of dynamic processes (Butt et al., 2005). The SUMO protease used for the cleavage of the tag, recognizes the conformation of the ubiquitin partner instead of the protein sequence, allowing efficient and accurate cleavage without adding extra residues (Butt et al., 2005).

A 6xHis-SUMO fusion construct can be used to enhance expression and aid purification of challenging proteins, and can be paired with Ni-NTA chromatography. Malakhov and colleagues (2004) constructed two fusions of the matrix metalloproteinase-13 (MMP13) protein, 6xHis-MMP13 and 6xHis-SUMO-MMP13, and expressed these constructs in *E. coli* (Malakhov et al., 2004). The 6xHis-MMP13 was detected as an insoluble aggregate, while the 6xHis-SUMO-MMP13 construct was mostly soluble. The investigators proposed that SUMO, when fused to

MMP, served as a molecular chaperone to aid solubility and increase purified protein yield (Malakhov et al., 2004).

1.5.3 The GST Fusion Tag

The 26 kDa glutathione S-transferase (GST) affinity tag can also be a viable method for inducible high-level protein expression and production from bacterial cell lysates (Harper and Speicher, 2011). This affinity tag has been applied in diverse fields, such as immunological studies, vaccine production, investigations of protein-protein interactions and structural determinations using NMR or crystallography. The GST moiety binds with high affinity to glutathione coupled to an agarose or Sepharose bead matrix (Harper and Speicher, 2011). The GST fusion protein can be eluted using reduced glutathione, under non-denaturing conditions and without the use of detergents. Removal of the GST tag can be done by re-chromatography on a glutathione column, and the target recombinant protein can be further purified using gel filtration or ion exchange (Harper and Speicher, 2011). Careful consideration must be given to determine whether the GST tag should be cleaved. If the oligomeric state of GST is presumed to influence the protein of interest, removal of the tag is advised (Harper and Speicher, 2011).

1.6 Objectives of the Current Study

Despite many hallmark discoveries in resolving the structure of the caveolar coat complex, there is still a dearth of data providing detailed molecular characterization of the coat proteins and their functional associations (Hansen and Nichols, 2010). Cavin-caveolin protein-protein interactions are thought to be responsible for caveolae generation, but the difficulty in co-precipitating the two proteins makes it hard to define their putative interaction precisely, and to map domains of each protein involved in binding. The physical and spatial assembly of cavins and caveolins during caveolae biogenesis are poorly characterized and remain areas requiring further insight (Ludwig et al., 2013; Hansen and Nichols, 2010).

Our lab is conducting a multi-level study to purify caveolar coat components in order to map associations between these proteins. Other lab members are trying to purify caveolin-1. I want

to purify cavin-1 for use in these binding studies. Previous lab members had shown that a GST-cavin-1 fusion construct expressed in BL21(DE33) available in the lab was expressed moderately well and was partially soluble. Higher protein expression was obtained when a 6x-His-SUMO-truncated-cavin-3 (lab number: DB1480) was tested. Initial tests on 6His-SUMO-truncated-cavin-3 had shown that the LIC vector was leaky, leading to background expression of truncated cavin-3, which may have been toxic to the bacterial host. It was difficult to obtain transformants and enough plasmid DNA for sequencing. However, using the BL21(DE3) pLysS strain yielded more truncated cavin-3, due to the addition of the pLysS plasmid, which reduced basal expression of heterologous genes.

For these reasons, I first made a 6x-His-SUMO-tagged full-length cavin-1 expressed in BL21(DE3) pLysS, for comparison with our existing GST-cavin-1. I wanted to generate a construct encoding 6His-SUMO-cavin-1 by cloning *E. coli*-optimized full length cavin-1 into the LIC SUMO 2S-T vector, which contained the 6His-SUMO fusion tag. Once successful cloning was confirmed, expression and solubility of the 6xHis-SUMO-cavin-1 fusion were compared to those of the previously generated GST-cavin 1 construct. The concentration of IPTG, temperature and length of incubation after induction, were tested to optimize protein expression conditions. After these conditions were determined, studies of binding and release of 6His-SUMO-cavin-1 from Ni-NTA resin were performed. The GST-cavin-1 construct in BL21(DE3) was revisited to test protein release from glutathione-agarose beads. Parameters, including temperature of incubation after IPTG induction, detergent type and bead concentration, were tested to enhance bead binding and GST-cavin-1 yield. Studies on both constructs were done on a small scale to evaluate expression and solubility of cavin-1, before choosing a method for scaling up to obtain purified cavin-1 for use in binding studies with caveolin-1. Performing such studies should increase understanding of the molecular and spatial dynamics of cavin-caveolin interactions and the possible mechanisms by which these complexes drive caveolae formation.

Chapter 2

METHODS AND MATERIALS

2.1 Cloning Full Length Codon-Optimized Cavin-1: Creating the 6xHis-SUMO Construct

The QuikChange ® method from Stratagene was used to introduce a restriction enzyme recognition site into the SUMO plasmid, pET His6 SUMO TEV LIC cloning vector (2S-T from Addgene), by site-directed mutagenesis to change the SSpI site, AATATT, to SpeI, ACTAGT. The forward primer mixture contained : 125 ng of forward primer, 100 ng of template SUMO plasmid (LIC SUMO vector 2S-T), 3 µl of dNTPs ,5 µl 10x buffer, and 0.5 µl of pfU Turbo. Distilled water was added for a total reaction volume of 50 µl. The forward primer (lab number: DB1490-1) had the sequence: GAAAACCTGTACTTCCAATCCACTAGTGGAAGTGGATAACGGATCCGC.

The reverse primer mixture contained: 125 ng of reverse primer, 100 ng of template SUMO plasmid (LIC SUMO vector 2S-T), 3 µl of NTPs, 5 µl 10x buffer, and 0.5 µl of pfU Turbo. Distilled water was added for a total reaction volume of 50 µl. The reverse primer (lab number: DB1490-2) sequence was: GCGGATCCGTTATCCACTTCCACTAGTGGATTGGAAGTACAGGTTTTC

The reaction mixtures were thermally cycled overnight in the thermal cycler (GeneAmp PCR System 2700, from Applied Biosystems) with the following cycle: 1 cycle at 95˚C for 30 seconds, 18 cycles each at 95˚C for 30 sec, at 62.2˚C for 1 minute, at 72˚C for 20 minutes, and 1 cycle at 72˚C for 20 minutes.

After PCR, 25 µl of each sample mixture for the forward and reverse primer were combined together in a 1.5 ml centrifuge tube (Clickseal microcentrifuge tubes, National Scientific Supply Co.), and 0.5 µl of pfU Turbo was added. Using the same PCR conditions, this new reaction mixture was thermally cycled overnight. After overnight PCR, 1 µl of Dpn1 restriction enzyme digest was added to the combined reaction tube (lab number: 1490-1/1490-2 PCR product) and incubated at 37˚C for 2 hours. The competent DH5 α bacteria tube was thawed and kept on ice. To this tube, 20 µl of the PCR product and DpnI mixture were added, and the contents were mixed well by pipetting and vortexing briefly. The total volume of this reaction mixture was approximately 100 µl. This reaction tube was heat shocked in a 42˚C

water bath for 45 seconds. Using a serological pipet, 400 µl of sterile LB broth was added to the mixture and pipetted 3 times to mix the contents. This mixture was transferred to 10 mL Falcon tubes and agitated on a shaker plate at a medium setting for 1 hour at 37˚C. An agar plate containing ampicillin (100 mg/ml) was streaked with this mixture of broth and bacteria, and incubated overnight. The following day, a transfer loop was used to transfer one distinct bacterial colony into each of two tubes containing 3 ml of LB broth. These culture tubes were incubated overnight at 37˚C. The AccuPrep Plasmid Mini Extraction Kit from Bioneer was used for the subsequent plasmid extraction for each culture tube, and 2 ml from each culture tube was used in the procedure. The concentration of each of the two plasmid extracts was checked using a BioSpec mini (Shimadzu Corp.) spectrophotometer at OD_{600}, and these extracts were sequenced. For the sequencing reactions for each, 0.5 µg of plasmid extract DNA from each tube was mixed with 3.2 pmol of sequencing primer (*S. cerevisiae* Smt3 SUMO+192F; sequence: CTCCTTAAGATTCTTGTACGACGG) in a sequencing tube. Distilled water was added to obtain a total reaction volume of 8 ul in each tube. PCR on cavin-1 was performed the following day, preparing reaction mixtures for the upstream cavin-1 full length forward (lab number: 1493_1Cavin-1 FL FW; sequence: GAGACTAGTATGGAAGACCCGAC), and downstream cavin-1 full length reverse (lab number: 1493_2Cavin-1 FL Rev; sequence: CGTGGATCCTTAATCAGAGTCAC) primers. These are *E. coli* optimized full length cavin-1 in the plasmid cloning vector pUC57 from GenScript. For each reaction tube, 15 pmol of each forward and reverse primer , 20 ng of optimized pET28 12His MBP TEV (EcoRI cavin 1 SalI *E. coli*, lab number: DB1477), 1 µl of 10 mM dNTPs, 5 µl of 10X pfU buffer, 0.5 µl pfU Turbo were mixed together. Distilled water was added to obtain a total reaction volume of 50 µl per tube. A total of three reaction tubes were prepared and these were thermally cycled overnight. The following program was used in the GenAmp thermal cycler: 1 cycle at 96˚C for 3 minutes, 32 cycles each at 94˚C for 30 seconds, at 54.5˚C for 30 seconds, at 72˚C for 1 minute 45 seconds, and 1 cycle at 72˚C for 5 minutes.

After thermal cycling, the three PCR mixtures were pooled together for the total PCR product. This PCR product was cleaned to get rid of excess dNTPs using a Zymoclean column, and eluted with 20 µl of 60˚C distilled water. The PCR product was digested using high-fidelity BamHI. For

the digestion mixture, 16 µl of PCR product, 2 µl of 10X NEB Buffer #4, 1 µl of high-fidelity BamHI and 1 µl of SpeI were combined in a 1.5 ml centrifuge tube. The digested product was run on an 0.8% agarose gel, and imaged. The visualized fragment was cut and eluted in the Zymoclean gel purification column, using 15 µl of 60˚C distilled water for the final elution step. Minipreps for DNA (lab number: DB1491) extraction using the Accuprep Mini Plasmid Extraction kit were done. The concentration of the DNA extraction was read at OD_{600}.

In a 1.5 mL centrifuge tube, 3 µg or 15 µl of DNA extract (lab number: DB1491, volume determined based on concentration), 2 µl NEB 10X Buffer #4, 1 µl SpeI, 1 µl Bam HI, and 1 µl H_2O were combined, and kept in a 37˚C water bath for 2 hours. This mixture of cut vector was run on a 0.8% agarose gel alongside a sample of uncut vector, and imaged. The gel fragment containing the cut vector was excised, cleaned with the Zymoclean column, and eluted with 30 µl 60˚C distilled water.

For the ligation mixture, 7 µl of the PCR product cut with SpeI/BamHI, 3 µl of the new vector DB1491 (cut with SpeI/Bam HI), 3µl 10X ligase buffer, 1 µl T4 ligase and 16 µl of distilled H_2O were combined. To ensure that the vectors were cut, one agar plate containing ampicillin (100 mg/ml) was prepared for vector and ligase as the control, and another plate for vector alone was prepared. For the vector and ligase plate, 3 µl of vector, 3 µl 10X buffer, 1 µl ligase, and 23 µl of dH_2O were combined. For the “vector alone” plate, 3 µl of vector, 3 µl 10X Buffer and 24 µl of dH_2O were combined. These plates were incubated overnight at 16˚C. For the transformation of the SUMO plasmid into competent bacteria BL21 (DE3) pLysS, the vector (DB1491) was combined with 15 µl of ligation mixture, re-suspended in 400 ml LB broth and incubated for 1 hour on the rocker at 37˚C. After 1 hour, 200 ml of the transformation mixture was spread on an agar plate containing ampicillin (100 mg/ml stock used for all experiments) and chloramphenicol (34 mg/ml stock used for all experiments), and incubated overnight. The plate was checked for transformants. A 5 ml culture with ampicillin used at 100 µg/ml and chloramphenicol used at 34 µg/ml (1:1000 dilutions of the aforementioned stock solutions) was prepared using 5 ml of LB broth and the transformed colony that grew on the agar plate. A mini-prep DNA extraction was performed on this transformed culture. The transformant extract

was sent for sequencing using the primer SC Smt3_SUMO +192F to ensure that the desired final construct was obtained. Once this was confirmed, a glycerol stock of the SUMO tagged cavin-1 in BL21 (DE3) pLysS (lab number: DB1493) was made for future cell culture preparations.

2.2 Tests for Expression and Solubility of 6His-SUMO-cavin-1 (Lab Number: DB1493)

Inoculation and Cell Culture Preparation for All DB1493 Tests (Including IMAC): For overnight culture preparations, ampicillin-resistant DB1493 was inoculated in 3 ml LB from the glycerol stock. Ampicillin used at 100 µg/ml and chloramphenicol used at 34 µg/ml were added (diluted from the aforementioned stock solutions). The sample was incubated overnight on a shaker at 37˚C. For one-20 ml culture, 18 µl of sterile LB broth and 2 ml of the overnight culture were added to a 125 ml Erlenmeyer flask. Ampicillin and chloramphenicol were added (20 ul of each) to the culture, at the dilutions indicated previously. Cells were grown at 37˚C on a shaker plate until OD_{600}=0.8, before induction with IPTG (from a 1 M stock solution), according to individual experimental requirements outlined in the following sections. Incubation temperature and length after induction are also described in the sections that follow.

Western Blot Analysis for All DB1493 Tests (Including IMAC): An 11% acrylamide gel was prepared for a 1.0 mm gel (from Bio-Rad) frame using 1.83 ml of acrylamide (with 8% bisacrylamide), 1.88 ml Tris pH 8.8, 1.23 ml of distilled water, 25 µl 20% SDS, 40 µl of 10% APS and 10 µl TEMED. Ethanol was poured on the running gel to eliminate air bubbles before placing in the 37˚C incubator to solidify. For the stacking gel, 1.825 ml distilled water, 312.5 µl Tris pH 6.8, 400 µl acrylamide (8% bisacrylamide), 12.5 µl of 10% APS, and 7 µl of TEMED were vortexed together in a culture tube and poured over the running gel. A 15-well comb from Bio-Rad was placed in the gel frame. The gel frame was kept in the incubator to solidify the stacking gel. The prepared gel was kept in SDS-PAGE running buffer. The SDS-SB lysed samples from experiments were boiled for 5 minutes at 100˚C on a hot plate. These samples were vortexed briefly, spun down for 2 minutes at 13200 rpm, diluted in 2X SDS-SB according to experimental requirements, and were loaded into the wells of the prepared gel (sample volumes and dilutions are included at the end of each individual experiment). A pre-stained protein ladder (Bio RAD Precision Plus Protein® Dual Color Standards) was loaded alongside the samples. The

gel was run at 100V until the ladder bands started to separate, at which point the voltage was increased to 200V for the remainder of the running time. The gel was washed in 1X Transfer Buffer (12.12g Tris, 57.6 g Glycine in 800 mL methanol) for approximately 15 minutes to remove salts. Separated proteins in the gels were electrophoretically transferred onto a PVDF membrane (Immobilon-P Transfer Membrane) at 100 amps for 1 hour. The blotted membrane was blocked for 1 hour in 10% non-fat milk in PBS containing Tween on a rocker at medium setting. For the primary antibody probe, the PVDF membrane was incubated for 1 hour at room temperature with mouse monoclonal anti-6x His (Pierce; 0.5 µg/µl concentration) diluted to 1:2000 in milk-PBS-T. The membrane was then thoroughly washed with PBS-T three times, once for 10 minutes on a rocker, and then two times for 5 minutes each, to remove excess or unbound antibody. For the secondary antibody probe, the bound antibodies on the membrane were detected by horseradish peroxidase-conjugated anti-mouse Ig secondary antibody (Jackson ImmunoResearch Laboratories) diluted to 1:4000 in PBS-T and incubated for 1 hour at room temperature. The membrane was then washed three times with PBS-T as before. An electrochemiluminescence (ECL) detection system (Perkin Elmer Western Lightning ECL) was used according to manufacturer's instructions before exposing the membrane to autoradiography film (BioExcell Autoradiographic Film). Exposures of several seconds to 1 hour were performed, until bands could be clearly visualized on the film. The film was developed using the AlphaTek AX 300 SE.

2.2.1 Four- hour time Course and Temperature Test Comparing Incubation at 29˚C and 37˚C After Induction

Cell Culture/Sample Prep for Time-Course: Two- 20 ml cultures were prepared. One flask was designated for a 29˚C test and the other for 37˚C. From one flask, 0.1 ml was removed as the "un-induced control sample", spun down for 4 minutes at 13200 rpm (using the Eppendorf centrifuge 415D), and re-suspended in 50 µl of 25 mM Tris-Cl (pH ~7.4). To the re-suspended mixture, 50 µl of 2x SDS-sample buffer (with 10% BME) was added, mixed thoroughly, and boiled on a hot plate for 5 minutes at 100˚C. This lysed sample was frozen at -20˚C. Both cultures were induced with 0.5 mM IPTG .The flask for 29˚C was briefly cooled over ice before

the IPTG was added. The 29˚C and 37˚C cultures were placed in incubators set to the appropriate temperature. At each time point of 1, 2, 3 and 4 hours, 0.1 ml aliquots of the cultures at each temperature were removed and placed in 1.5 ml centrifuge tubes. These aliquots were spun down for 4 minutes at 13200 rpm, re-suspended in 50 ul of 25 mM Tris-Cl (pH ~7.4) and lysed with 50 µl of 2X SDS-SB (with 10% BME). These time-course samples were frozen at -20˚C.

Extractions for Solubility Test: Prior to the 4th 1-hour long incubation, 400 µl of cell culture were removed from each Erlenmeyer flask and placed into two new 10 ml Falcon tubes (to reduce sample volume loss from evaporation). After removing the 0.1 ml aliquots at end of the 3 hour collection point, 19 ml of each culture (29˚C and 37˚C) were removed and placed in 50 ml Oak Ridge conical tubes to test for the solubility of the protein. The cells in the tubes were spun down in a cooled centrifuge (Sorvall RC-5 Superspeed Refrigerated Centrifuge, DuPont Instruments) at 5000 rpm for 10 minutes at 4˚C. The resulting supernatants for each culture were discarded and the remaining cell pellet in each tube was re-suspended in 400 µl of Native Lysis Buffer (defined as 50 mM Hepes at pH 7.5, 400 mM NaCl, 100 mM KCl, 5% glycerol). The following protease inhibitors were added: 1 µg/ml of leupeptin (1 mg/ml stock) and pepstatin (1 mg/ml stock) each, and PMSF added to 0.5 mM from a 100 mM PMSF in EtOH stock solution. The suspension was pipetted up and down several times to properly disperse the cell pellet and homogenize the contents of the tube. Lysozyme was added to the cell suspension to 0.5 mg/ml from a 50 mg/ml stock (made in a 1:1 mixture of Native Lysis Buffer and glycerol). Triton X-100 was added to 1% from a 10% stock solution in water. These suspensions were transferred to new 1.5 ml centrifuge tubes and incubated for 45 minutes on an end-over-end tube rotator at 4˚C. After incubation, the lysates were sonicated over ice with a micro-tip sonicator (Branson Sonifier Cell Disruptor 185) 6 times, 10 seconds each time, with 15 second pauses in between each sonication (output control:5, Power: 20-40 units). The lysates were centrifuged for 10 minutes at 1600 rpm in a microfuge at 4˚C. Supernatants containing the total soluble fraction of protein were stored in new 1.5 ml centrifuge tubes. Five microliters from each total soluble fraction were prepared for SDS-PAGE, by re-suspending samples in 5 µl of 2x SDS-SB. The remaining pellets in each of the tubes were re-suspended in 200 µl of 2x SDS-SB. This was the

insoluble fraction sample prepared for SDS-PAGE. The total soluble fractions (not for the gel) were flash-frozen in liquid nitrogen and stored at -90˚C for subsequent use in the first IMAC test (see section 2.3.1).

Sample Volumes/Dilutions for SDS-PAGE: For each time course and solubility test sample, 1 µl of 1:10 dilutions (in 2X SDS sample buffer) were loaded into the wells.

2.2.2 Second Test of SUMO-cavin-1 Solubility

Approach 1/Extracting in a Larger Sample Volume (Performed Twice): Two 20 ml cultures were incubated for 3 hours at 37˚C after induction with 0.5 mM IPTG. Cultures were transferred to two Oak Ridge tubes and spun down at 5000 rpm for 5 minutes at 4˚C to pellet. The cell pellets were pooled together in a 50 ml Erlenmeyer flask after re-suspension in 35 ml of Native Lysis Buffer. The pooled suspension was sonicated over ice with a Branson Sonifier Analog Cell Disruptor 250-450 (output value of 7.5, and 50% duty), using the same sonication and rest cycle as before. Triton X-100 was added to the lysate to a final concentration of 1%. The lysate was transferred to two Oak Ridge tubes and centrifuged at 15,000 rpm for 30 minutes at 4˚C (Sorvall refrigerated centrifuge). The supernatant containing the total soluble fraction was transferred to a new 50 ml Falcon tube. Fifty microliters of total soluble protein were transferred into a new 1.5 ml centrifuge tube, and samples were lysed in 50 µl 2X-SDS SB. The remaining cell pellet containing the insoluble fraction was re-suspended in 200 µl 2X-SDS SB. For SDS-PAGE, 20 µl of the soluble (diluted in 1:1 2X SDS-SB) and 5.7 µl of a 1:100 dilution for the insoluble fraction were loaded.

Approach 2 (Performed by Other Researcher)/Comparing Solubilization with Fos choline-16 and Triton X-100: Two 20 ml cultures were incubated for 3 hours at 37˚C after 0.5 mM IPTG induction. Cultures were transferred to two Oak Ridge tubes and spun down at 5000 rpm for 5 minutes at 4˚C to pellet. Each pellet was re-suspended in 400 µl Native Lysis Buffer (with protease inhibitors), as before. To one tube, Triton X-100 was added to a final concentration of 1%, while the other tube was supplemented with Fos choline-16, to a final concentration of 1%. The tubes were incubated for 5 minutes, on ice. The lysates were centrifuged at 1600 rpm at 4 ˚C in a microfuge. Supernatants containing total soluble fractions of protein were transferred to

centrifuge tubes. Twenty microliters of each soluble fraction were lysed in an equal volume of 2X SDS-SB. The remaining cell pellet containing the insoluble fraction was lysed with 200 µl 2X-SDS SB. For SDS-PAGE, two microliters of a 1:10 dilution of total soluble fractions (prepared in 2X SDS-SB) and five microliters of a 1:100 dilution of the insoluble fractions were loaded on the gel. Results are shown in Figure 3.

2.2.3 Test 6His-SUMO-cavin-1 Expression and Solubility with 0.1 and 0.5 mM IPTG Inductions and Incubation at 16˚C

Cell Culture/Time-Course Sample Prep: Four- 20 ml cultures were prepared. Two cultures were induced with 0.1 mM IPTG (one of which was selected for overnight incubation), and two other cultures were induced with 0.5 mM IPTG (one of which was selected for overnight incubation). All cultures were incubated at 16˚C after induction. At each time point of 1, 2, 3 and 4 hours, a 0.1 ml aliquot from 0.1 mM and 0.5 mM IPTG culture flasks was collected and prepared for SDS-PAGE, as in 2.2.1. For the 4th 1-hr incubation for the non-overnight flasks, 600 µl of each culture was conserved in the Erlenmeyer flask (to reserve enough sample, even after evaporation). The two other flasks were kept in the incubator overnight.

Extractions for Solubility Test: After the 3rd time point, 18 ml of the 0.1 mM and 0.5 mM cultures were spun down in 50 ml Oak Ridge conical tubes. Cell pellets were re-suspended in 360 ul of Native Lysis Buffer. Protease inhibitors and lysozyme were added, at the same concentrations as before. Cell suspensions were incubated for 25 minutes at 4˚C. Fos choline-16 was added to the samples to a final concentration of 1% (40 µl). The lysates were incubated at 4˚C for 30 minutes on an end-over-end rotator, sonicated with the micro-tip sonicator, and centrifuged, as before. Total soluble and insoluble fractions were prepared for SDS-PAGE, as before. The overnight cultures were prepared for the solubility test in the same way. The remaining soluble extracts for each of the four cultures were used for IMAC (see section 2.3.2).

Sample Volumes/Dilutions for SDS-PAGE: One µL of time course samples, 5 µl of 1:100 dilutions of soluble samples and 6.25 µl of 1:500 dilutions of insoluble fractions were loaded.

2.3 IMAC Tests for Binding and Elution of 6His-SUMO-cavin-1 from Ni-NTA Beads

2.3.1 First IMAC Test on Solubility Test Samples (From 2.2.1)

Bead Washes and Elutions: Nickel-NTA (His Pur® Ni-NTA Resin, Thermo Scientific) beads were re-suspended by vigorously shaking the suspension in the bottle, and 300 µl of bead suspension (for 150 µl packed beads) were pipetted into a clean 1.5 ml centrifuge tube. The beads were washed three times with high salt wash buffer (HSWB, defined as 50 mM phosphate buffer, pH 8.0, 300 mM NaCl, 10% glycerol, 1% Triton X-100), with 1 ml of buffer for each wash. Each wash was supplemented with protease inhibitors 0.5 mM PMSF, 1 µg/ml leupeptin, and 1 µg/ml pepstatin. Imidazole from a 5 M imidazole stock solution (in phosphate buffer and 1% Triton X-100, pH 8.0), was added to a final concentration of 10 mM. After adding each wash solution to the bead pellet, the tube was spun down in the centrifuge for 3 minutes at 13200 rpm. The wash supernatants were discarded in between washes. For the last wash, the bead suspension was divided into 2 equal parts in new 1.5 ml centrifuge tubes, one designated for the 29˚C soluble extract, and the other for the 37˚C extract. Remaining supernatants were discarded. The frozen soluble extracts for 29˚C and 37˚C (from the solubility test in 2.2.1) were thawed and transferred to the bead pellet in the centrifuge tube. The tubes were incubated for 1 hour at 4˚C in an end-over-end tube rotator. After incubation, the tubes were spun in the microfuge for 1 min. From the supernatants containing the unbound fractions, 50 µl were transferred to new 1.5 centrifuge tubes for SDS-PAGE, lysed with an equal volume of 2x SDS-SB. This was the “unbound protein”. The Ni-NTA beads containing the bound protein were rinsed three times with Wash Buffer-10 (WB-10), defined as HSWB, pH 8.0. containing 10 mM imidazole (supplemented with protease inhibitors, as before), using 1 ml of buffer for each wash. Each wash was spun down in the centrifuge for 3 minutes at 13200 rpm, and wash supernatants were discarded as previously indicated. Beads containing bound protein were washed with 200 µl of Wash Buffer-50 (WB-50), defined as HSWB pH 8.0 with 50 mM imidazole (supplemented with protease inhibitors, as before) were added. The bead tubes were incubated for 10 minutes at room temperature on an end-over-end tube rotator, and spun in the centrifuge for 1 minute at 13200 rpm. Supernatants containing the 50 mM imidazole-washed protein were transferred

to new centrifuge tubes, and lysed with 200 µl 2x SDS-SB. This was the "WB-50 protein". The beads containing bound protein were eluted with 200 µl of Elution Buffer-250, defined as HSWB pH 7.0 with 250 mM imidazole (supplemented protease inhibitors) were added, and incubated as before. The collected eluate from the first 250 mM imidazole elution was "EB-250-1". Samples were eluted a second time with EB-250 (EB-250-2). Eluates from each EB-250 elution were prepared for SDS-PAGE by lysis in 200 µl SDS-SB.

Sample Volumes/Dilutions for SDS-PAGE: One microliter of 1:10 dilutions (in 2x SDS-SB) of unbound, WB-50, EB-250-1 and EB-250-2 samples were loaded on the gel.

2.3.2 IMAC Binding Test, Substituting Fos choline-16 (0.00053%) for Triton X-100 in Washes and Elutions

Bead Washes and Elutions: Four tubes of beads, each containing 75 µl Ni-NTA beads, were washed, as before, with HSWB without any Triton X-100. The four frozen soluble extracts, 0.1 mM IPTG-induced, 0.1 mM IPTG-induced overnight (O/N), and their 0.5 mM IPTG-induced equivalents (from section 2.2.3) were thawed and transferred to the washed bead pellets. Imidazole from a 5M imidazole stock solution (in phosphate buffer, pH 8.0, no Triton X-100) was added to each thawed extract for a final concentration of ~10 mM. The samples were incubated as before, and the unbound fractions were collected for SDS-PAGE. The wash buffers, WB-10 and WB-50 and the elution buffer, EB-250, were prepared as before but using imidazole without any Triton X-100. All subsequent wash and elution steps were adjusted to contain 0.00053% Fos choline-16 (to achieve 2.5 times the critical micelle concentration). The beads were washed with WB-10, and WB-50, and eluted twice with EB-250.

Sample Volumes/Dilutions for SDS-PAGE: For all 0.1 mM IPTG-induced samples, 5 µl of 1:100 dilutions were loaded. For the 0.5 mM IPTG-induced overnight (O/N) samples, 5 µl and 15 µl of 1:100 dilutions of each sample were loaded.

2.3.3 IMAC with Increased Fos choline-16 Concentration (0.1%) in Washes and Elutions, and an N-lauroyl sarcosine-Supplemented Imidazole Elution

Cell Culture and Extraction: One 20 ml culture was induced with 0.5 mM IPTG, after cooling the flask on ice for a few minutes. The cells were grown for 4 hours at 16˚C. The culture was transferred to a 50 ml conical Oak Ridge tube, and spun down for 10 minutes at 5000 rpm at 4˚C to pellet. The cell pellet was re-suspended in 360 ul of Native Lysis Buffer. Protease inhibitors and lysozyme were added, at the same concentrations as before. The cell suspension was incubated for 45 minutes at 4˚C. Fos choline-16 was added to 1% (40 µl). The lysate was incubated at 4˚C for 30 minutes, sonicated with the micro-tip sonicator, and centrifuged. Fifty microliters of soluble supernatant and the insoluble pellet were each prepared for SDS-PAGE.

Bead Washes and Elutions: One centrifuge tube containing 150 µl of Ni-NTA bead suspension was washed as before, using HSWB but without any Triton X-100. The remaining soluble supernatant was incubated with the Ni-NTA beads, as before. All subsequent wash buffers and elution buffers, WB-10, WB-50 and EB-250, were prepared with imidazole without Triton X-100. Fos choline-16 was added to a final concentration of 0.1% to each buffer. The beads were washed, as before, with WB-10, and WB-50, and eluted once with EB-250. Two 400 µl elutions were done using an elution buffer containing N-lauroyl sarcosine. This elution buffer was made like EB-250, but with the addition of 0.1% N-lauroyl sarcosine from a stock solution of 1% N-lauroyl sarcosine in 50 mM Tris, pH 8.0.

Sample Volumes/Dilutions for SDS-PAGE: For all samples, 7.5 µl of 1:50 dilutions were loaded.

2.3.4 Testing Elution with EDTA to Release Protein from Ni-NTA Beads

One 20 ml culture was induced with 0.5 mM IPTG. The cells were grown for 4 hours at 16˚C and pelleted. The cell pellet was re-suspended in 360 µl of Native Lysis Buffer (with added protease inhibitors and lysozyme, as before) and incubated for 45 minutes at 4˚C. Fos choline-16 was added to 1% (40 µl). The lysate was incubated, sonicated and centrifuged, as before. Insoluble and soluble fractions were prepared for SDS-PAGE. IMAC washing and elution conditions for the remaining soluble extract were the same as in section 2.3.3. A final elution

was performed using elution buffer containing EDTA. This elution buffer was made from 360 µl of EB-250 and 40 µl of 0.5 M Na_2EDTA (pH 8.0) stock solution, for a final elution volume of 400 µl. The tube was incubated for 5 minutes at room temperature before being spun down for 1 minute at 13200 rpm. The eluate was transferred to a new tube and prepared for SDS-PAGE. For all samples, 7.5 µl of 1:50 dilutions were loaded onto the SDS-PAGE gel.

2.4 Tests on the GST –cavin-1 Construct (Lab Number: DB1298)

Inoculation and Cell Culture Preparation for All DB1298 Tests: An overnight culture of plasmid GST cavin-1 in BL21(DE3) (with ampicillin used at 100 µg/ml) was inoculated in 3 ml LB from the glycerol stock. One 20 ml culture was prepared with 18 ml of LB broth and 2 ml of the overnight culture. Ampicillin (100 mg/ml stock) was used at 100 µg/ml. Cells were grown at 37˚C on a shaker plate until OD_{600}=0.8, before induction with 0.5 mM IPTG (from a 1 M stock solution). After incubation after induction (temperature and duration outlined according to individual experiments), the culture was transferred to a 50 ml conical Oak Ridge tube, and spun down for 10 minutes at 5000 rpm at 4˚C to pellet.

Extraction of Cell Pellet for DB1298 Experiments: The cell pellet was re-suspended in 400 µl Native Lysis Buffer and protease inhibitors PMSF, leupeptin and pepstatin, were added to final dilutions as indicated previously. Lysozyme was added to the cell suspension, as before. The sample tube was incubated for 1 hour at 4˚C, and sonicated with a micro-probe sonicator, with the routinely used cycles. Triton X-100 was added to a final concentration of 1%. The lysate was incubated for 5 minutes at 4˚C, on the end-over-end rotator and centrifuged at 1600 rpm at 4˚C. Soluble and insoluble fractions were prepared for SDS-PAGE. Modifications to this procedure are included in individual experiment descriptions.

Western Blotting Analysis for All DB1298 Experiments : Gels and samples for SDS-PAGE were prepared as in the tests with 6His-SUMO-cavin-1. Electrophoretic transfer to a PVDF membrane was performed as before. For the primary antibody probe, the membrane was incubated overnight at 4˚C with pAb anti-PTRF (IgG Purified Rabbit Sera LYOPH, from NOVUS) diluted to 1:250 in milk-PBS-T. The membrane was then thoroughly washed with PBS-T three times, once for 10 minutes on a rocker, and then two times for 5 minutes each. For the secondary antibody

probe, the bound antibodies on the membrane were detected by horseradish peroxidase-conjugated anti-rabbit Ig secondary antibody (Jackson ImmunoResearch Laboratories) diluted to 1:4000 in PBS-T and incubated for 1 hour at room temperature. The membrane was then washed three times with PBS-T as before. ECL and film exposures were done as before.

2.4.1 First Test of GST-cavin-1 Binding and Release from Glutathione-Agarose Beads

Cell Culture and Extraction: One 20 ml culture was prepared. The cells were grown for 4 hours at 37˚C after induction, pelleted and extracted.

Bead Binding: Glutathione-Agarose beads (from Pierce) were re-suspended by swirling, and 50 µl of bead suspension were transferred to a fresh 1.5 ml centrifuge tube. The beads were washed three times with Native Lysis Buffer, using 1 ml for each wash. The beads were spun down for 2 minutes at 13200 rpm for each wash, and wash supernatants were discarded. The bacterial lysate containing the total soluble fraction was transferred to the bead column, and incubated for 2 hours at 4˚C, on the end-over-end tube rotator. The lysate was spun down for 1 minute at 13200 rpm. The supernatant containing the unbound fraction was transferred to a new centrifuge tube for the next experiment (see section 2.4.2), and 50 µl of the unbound fraction was lysed with 17 µl of 4x SDS-SB for SDS-PAGE (unbound protein sample). The beads containing bound protein were rinsed 3 times with Native Lysis Buffer as before. The supernatants were carefully removed using a 1 ml syringe with a 25 gauge needle (from BD), to prevent disturbance to the beads. To the tube of beads, 150 µl of glutathione elution buffer, defined as 50 mM Tris Cl, pH 8.0, 10 mM freshly added reduced L- glutathione (Sigma-Aldrich) and 0.1% N-lauroyl sarcosine (in 50 mM Tris, pH 8.0), were added. The sample was incubated for 20 minutes at room temperature, on an end-over-end rotator. The tube was flicked lightly to mix the sample after 10 minutes, before returning it to the rotator to complete the incubation. The lysate was spun down for 1 minute at 13200 rpm. The supernatant containing the glutathione-eluted protein was transferred to a new centrifuge tube for future use, while 50 µl of this fraction was saved for the gel, lysed with 17 µl of 4x SDS-SB (glutathione-eluted protein sample). The beads were washed with 0.5 ml 50 mM Tris pH 8.0, and spun down for 1

minute at 13200 rpm. The wash supernatant was discarded. The remaining pelleted beads were mixed with 200 µl 2X SDS-SB (SDS-beads sample).

Repeated Experiment with Modified Elution Time: The first GST-cavin-1 test was repeated. After the addition of glutathione elution buffer, the beads were incubated for 30 minutes, instead of 20 minutes.

Samples/Dilutions for SDS-PAGE: For the total soluble and unbound fractions, 5 µl of 1:10 dilutions were loaded. For the glutathione-eluted fraction, 4 µl of a 1:20 dilution, and for the SDS-beads sample, 5 µl of a 1:20 dilution were loaded.

2.4.2 Testing a 16˚C Incubation, Increased Bead Volume, and Re-incubation of the Unbound Fraction from 2.4.1 for GST-cavin-1

Cell Culture and Extraction: Two- 20 ml cultures were prepared. Cultures were grown for 4 hours after induction, one culture at 16˚C, and the other at 37˚C (which was labeled as the 3X-beads sample). The cells were pelleted, and extracted as indicated.

Bead Binding: For the 16˚C lysate and remaining unbound fraction from section 2.4.1, 50 µl of glutathione-agarose bead suspension were transferred to two 1.5 ml centrifuge tubes. The beads were each washed 3 times with 1 ml Native Lysis Buffer as before. For the 3X-beads sample, 150 µl of bead suspension (thrice the usual bead volume) were transferred to a centrifuge tube, and washed 4 times with 1 ml Native Lysis Buffer. All three tubes containing the beads and respective lysate were incubated for 2 hours at 4˚C, on the end-over-end rotator. Unbound fractions were prepared and saved as before. The two beads pellets containing the bound protein, for the 16˚C and the repeat unbound protein samples, were washed 3 times with Native Lysis Buffer as before, while the 3X-beads sample was washed 4 times. After the washes, 150 µl of glutathione elution buffer were added to the two bead pellets containing the 16˚C and repeated unbound samples. For the 3X-beads sample, 250 µl of this same elution buffer were added. All the samples were incubated for 20 minutes at room temperature on the end-over-end rotator, and flicked briefly after every 5 minutes to ensure proper mixing. Samples were spun down for 1 minute at 13200 rpm and the supernatants containing the

glutathione-eluted protein were transferred to new centrifuge tubes. Fifty microliters of each eluate were prepared for running on a gel, using 17 µl of 4X SDS-SB for lysis.

Samples/Dilutions for SDS-PAGE: For SDS-PAGE, 5 µl of 1:10 dilutions of all unbound samples, 4 µl of 1:20 dilutions of glutathione-eluted fractions (for 16˚C and re-incubated unbound), and 6.7 µl of a 1:20 dilution of glutathione-eluted protein for the 3X-beads sample were loaded on a gel.

2.4.3 Testing a Combined 29˚C and 2 hour Incubation After Induction

Cell Culture and Extraction: Two- 20 ml cultures were prepared and grown for 2 hours at 29˚C. Cell pellets were extracted as before. Lysates were pooled together.

Bead Binding: Beads were washed with Native Lysis Buffer and the pooled lysate was incubated with the glutathione-agarose beads, as before. To the beads containing the bound protein, 600 µl of glutathione-elution buffer was used for elution. From the total eluate, 50 µl were reserved for the gel, and lysed with an equal volume of 2X SDS-SB (glutathione-eluted protein). The bead pellet was washed with 0.5 ml Tris pH 8.0, and spun down for 1.5 minutes at 13200 rpm. The wash supernatant was discarded, and 200 µl 2X SDS-SB were added to the bead pellet (SDS-beads sample).

Samples/Dilutions for SDS-PAGE: Five microliters of 1:10 dilutions for the total soluble and unbound fractions were loaded on the gel, while 16 µl of the glutathione-eluted protein and 5.33 µl of the SDS-SB bead fraction were loaded.

2.4.4 Comparing Solubilization of GST-cavin-1 with Different Detergents, Triton X-100 and Fos Choline-16

Cell Culture and Extraction: Two cultures prepared and grown for 2 hours at 29˚C after induction. Cells were pelleted, as before. One cell pellet (Triton X-100 sample) was extracted as before. The other cell pellet (Fos choline-16 solubilized sample) was extracted as before, but substituting Triton X-100 with Fos choline-16 for a final 1% concentration.

Bead Binding: For the Triton X-100 sample, glutathione-agarose bead washes and incubations were performed as in previous experiments. For Fos choline-16 designated sample, Fos-choline 16 was added to a final concentration of 0.1% for all washes and elutions. For both samples, the final elution was performed with 600 µl of glutathione-elution buffer.

Samples/Dilutions for SDS-PAGE: Five microliters of 1:10 dilutions for the total soluble and unbound fractions were loaded on the gel, while 16 µl of the glutathione-eluted protein and 5.33 µl of the SDS-SB bead fraction were loaded.

2.4.5 2L Preparation of GST-cavin-1

Cell Culture and Extraction: A 20 ml overnight culture of GST-cavin-1 in BL21(DE3) was prepared from the glycerol stock. Two large flasks containing 1 L LB broth in each were warmed overnight at 37˚C. The following day, ampicillin was added to 100 µg/ml in each flask. To each flask, 5 ml of overnight culture were added and cells were grown at 37˚C until OD_{600}= 0.8. The cultures were induced with 0.5 mM IPTG and grown for approximately 3 hours at 37˚C. The cell cultures were evenly distributed among bottles with approximately 450 ml capacity, and spun down for 30 minutes at 5000 rpm at 4˚C. The supernatants were discarded. To one bottle of cell pellet, 15 ml of Native Lysis Buffer was added to re-suspend the cells. A sterile 10 ml serological pipet was used to pipet the suspension up and down to homogenize the mixture and disperse the pellet. This suspension was transferred to all the bottles to re-suspend the cells. Another 15 ml of Native Lysis Buffer was added to the first bottle to release any residual cells from the bottle. The re-suspended cell fractions were all pooled together in one bottle. The pellet and lysis buffer mixture was transferred to a 50 ml glass beaker (Pyrex) on ice. The cells were sonicated 3 times, using the Branson 250-450 Sonifier Analog Cell Disruptor, set to an output value of 7.5, and 50% duty. Each sonication was done for 1 minute, with a 5 minute pause in between. From the lysate, 50 µl of this whole cell lysate were saved for the gel, and prepared with 50 ul 2X SDS-SB. The remaining lysate was transferred to a 50 ml Oak Ridge tube and spun down at 15000 rpm for 30 minutes at 4˚C (Sorvall refrigerated centrifuge). From the supernatant containing the clarified cell lysate, 50 µl were saved for the gel and lysed with 50 µl 2X SDS-SB. The insoluble

cell pellet was dissolved in 200 µl 2X SDS-SB. The remaining clarified cell lysate was transferred to a 50 ml Eagle brand tube for the bead binding step.

Bead Binding: One hundred microliters of glutathione-agarose bead suspension were transferred to a centrifuge tube. The beads washed with 1 ml Native Lysis Buffer three times, and wash supernatants were discarded. Approximately 1-2 ml of clarified cell lysate was taken from the Eagle brand tube to re-suspend the glutathione-agarose beads for easy transfer back into the Eagle brand tube containing the clarified cell lysate. The tube was incubated for 2 hours at 4˚C on the end-over-end rotator. After the 2 hour incubation, the lysate was spun down in a cooled table-top centrifuge (Eppendorf Centrifuge 5810) for 10 minutes at 1811 g-force at 4˚C. The supernatant containing the unbound fraction was removed, while 50 µl of the sample were prepared with 17 µl 4x SDS-SB for the gel. The beads were transferred to a 15 ml Eagle brand conical tube in a total of 10 ml Native Lysis Buffer. The beads were centrifuged at 3000 rpm for 5 minutes at room temperature. The wash supernatant was discarded and the wash procedure was repeated two more times. The beads were re-suspended in 1.5 ml Native Lysis Buffer to remove as many beads from the conical tube as possible and transferred to a new 1.5 ml centrifuge tube. These beads were centrifuged for 1 minute at 13200 rpm and the wash supernatant was discarded, after being carefully removed using a 1 ml syringe with a 25 gauge needle, so as not to disturb the beads. To the beads, 1.5 ml of glutathione-elution buffer was added. The beads were incubated for 30 minutes at room temperature, on the end-over-end rotator. From the eluate, 50 µl sample were saved for the gel, and lysed with 17 µl 4X SDS-SB. The beads were rinsed once with 0.5 ml 50 mM Tris pH 8.0, and spun down as before, with the wash supernatant discarded. The bead pellet was re-suspended in 500 µl 2x SDS-SB.

Sample Volumes/Dilutions for SDS-PAGE: One microliter of 1:10 dilutions were loaded on the gel for the insoluble, soluble and unbound fractions. Two microliters of a 1:10 dilution for the glutathione-eluted protein, and 1.4 µl of a 1:20 dilution for the SDS-SB bead sample were loaded on the gel.

Coomassie Gel: On an acrylamide gel, BSA was loaded for 0.2, 0.5, 1, and 2 µg of protein, using 2X SDS-SB to dilute the BSA stock solution to the desired concentrations. Two, 5, and 10 µl of

the glutathione-eluted protein were loaded in the adjacent lanes. Standard protocol for staining and de-staining (de-stain: 30% methanol, 10% acetic acid) the Coomassie gel was followed. The Coomassie gel was kept in de-staining solution overnight. Bands were visualized over UV-light (see Figure 15).

2.5 Test Binding of GST-cavin-1 to 6His-caveolin-1

Bead Binding: Two hundred microliters of Ni-NTA bead slurry were transferred to each of two 2 ml centrifuge tubes. One tube was designated as the control, and the other was the experimental sample. The beads were washed three times each with 1 ml of TBS (defined as 20 mM Tris Cl, pH 8.0, with 200 mM NaCl), with 1.5 minute spins at 13200 rpm. The wash supernatants were discarded. One eluted 6His-caveolin-1 and one GST-cavin-1 sample was thawed. Thirty microliters of each starting material were mixed with 30 µl 2X SDS-SB, for SDS-PAGE (cavin-1 and caveolin-1 starting materials).

Experimental Cavin1/CAV1 Contents (Sample #1): To one washed bead pellet, the following were added: 250 µl of thawed caveolin-1, 350 µl of thawed cavin-1, 650 µl of TBS (20 mM Tris Cl, pH 8 + 200 mM NaCl). The mixture was brought to 0.00053% Fos choline 16 from a 10% stock solution, and 0.1% N-lauroyl sarcosine from a 1% stock of N-lauroyl sarcosine in Tris pH 8.0.

Control Tube Contents (Sample #2): To the washed bead pellet, the following were added: 250 µl of Ni-NTA Elution Buffer (TBS (pH 7.0)+ 200 mM NaCl + 250 mM imidazole, containing 1% Triton X-100), 350 µl of thawed cavin-1 , 650 µl of TBS (20 mM Tris Cl, pH 8 + 200 mM NaCl). The mixture was brought to 0.00053% Fos choline-16 from a 10% stock solution, and 0.1% N-lauroyl sarcosine from a 1% stock solution of N-lauroyl sarcosine in Tris, pH 8.0 .

The two tubes were incubated for 2 hours at room temperature on the end-over-end rotator. The samples were spun down for 1 minute at 13200 rpm. From the supernatants containing unbound fractions, 50 µl of each were saved for SDS-PAGE (unbound protein samples). The beads containing bound protein were washed three times with 1.5 ml of wash buffer containing 25 mM Tris Cl, 300 mM NaCl, 0.00053% Fos choline 16 and 0.1% N-lauroyl

sarcosine. Wash supernatants were discarded. To each tube, 400 µl of elution buffer prepared with 25 mM Tris Cl (pH 7.0), 200 mM NaCl, 250 mM imidazole, 0.00053% Fos choline 16 and 0.1% N-lauroyl sarcosine were added. The samples were incubated for 10 minutes at room temperature, on the end-over-end rotator, and spun down for 1 minute at 13200 rpm. The supernatants containing the imidazole- eluted fractions were saved in new 1.5 ml centrifuge tubes. From these, 50 µl of each were transferred to fresh tubes, and lysed with 50 µl 2X SDS-SB for SDS-PAGE.

Western Blot Analysis: For one SDS-PAGE gel, the following were loaded in this order: 0.25 µl Caveolin-1 starting material, 1 µl imidazole-eluted fraction of control sample (undiluted), 1 µl imidazole –eluted fraction of experimental sample (undiluted), 1 µl re-loaded imidazole-eluted fraction of the control. Transfer and blocking conditions were kept the same. The membrane was incubated overnight with anti-caveolin-1 pAb (BD Transduction Laboratories, 250 µg/ml, catalog #: 610060) at a 1:1000 dilution in milk-PBST. For another SDS-PAGE gel, the following were loaded in this order: 0.02 µl cavin-1 starting material, 0.1 µl cavin-1 starting material, 2 µl imidazole-eluted fraction of the experimental (undiluted), 2 µl imidazole-eluted fraction of the control (undiluted), 10 µl undiluted imidazole-eluted fraction of the experimental and 10 µl undiluted imidazole-eluted fraction of the control. Transfer and blocking conditions were kept the same. This latter membrane was probed overnight with pAb anti-PTRF at the same 1:1000 dilution. Both membranes were washed three times with PBS-T after each antibody probe, as before, to get rid of unbound and excess antibody. ECL and film exposures were performed as indicated.

Chapter 3

RESULTS

The first objective in this study was to generate a plasmid encoding 6His-SUMO-cavin-1 by cloning full length cavin-1 into the LIC SUMO vector, which contained the 6His-SUMO fusion tag. The Quikchange method was used to introduce an in-frame cloning site downstream of the SUMO sequence and TEV site in LIC SUMO vector 2S-T, to change the SspI site to an SpeI site (lab number: DB1491). The desired mutation was verified by sequencing. The *E. coli* strain, BL21 (DE3) pLysS, was chosen for the expression of the desired recombinant protein. The added pLysS plasmid produces T7 lysozyme, which reduces basal expression of the T7-driven heterologous genes (Life Technologies, 2010), such as the recombinant gene of interest. In previous cloning experiments for cavin-3 constructs conducted in the lab, the SUMO vector was found to be leaky, leading to background expression of the protein, which may be toxic to the bacterial cells. In this cavin-1 study, the BL21 (DE3) pLysS strain would repress basal expression of this foreign protein, prior to induction with IPTG in later protein expression steps. Based on the growth of one colony on the ampicillin-agar plates after transforming the 6His-SUMO-cavin-1 into competent BL21(DE3) pLysS with the ligation mixture (made of the PCR product digest and cut vector, whose sizes were confirmed through visualization on the agarose gel), it was assumed that the desired recombinant plasmid was obtained. To confirm this, the plasmid DNA from this colony was sequenced. Successful insertion of the cavin-1 cDNA into the 6His-SUMO vector was verified by sequencing.

The following sequence was obtained for the desired 6 His SUMO cavin-1 construct (lab number: DB1493):

AATATAATTCTAGCCTGAATCAGACCCCCTGAAGATTTGGACATGGAAGGATAACGATATTATTGAGGC
TCACAGAGAACAGATTGGTGGGATCGAGGAAAACCTGTACTTCCAATCCACTAGTATGGAAGACCCGAC
GCTGTACATTGTTGAACGCCCGCTGCCGGGCTACCCGGACGCCGAAGCGCCGGAACCGAGCAGTGCAG
GTGCCCAGGCAGCAGAAGAACCGTCTGGTGCAGGTAGTGAAGAACTGATCAAATCTGATCAAGTTAAC
GGCGTCCTGGTGCTGAGTCTGCTGGACAAAATTATCGGTGCTGTCGATCAGATTCAACTGACCCAGGCG
CAACTGGAAGAACGTCAGGCTGAAATGGAAGGCGCGGTGCATTCGATCCAAGGCGAACTGATCAAACT
GGGTTAAGCCCATTCAACCACGTCCAACACCGTGTCAAAACTGCTGGAAAAAGTTCGCAAAGTTTCGGT
CAATGTGAAAACGGTGCGTGGCAGCCTGGAATGTCAGGCAGGTTAAATCAAAAAACTGGATGTTAACG

AATCAGAACTGCTGCTTCTCCGTAACTTCAAAGTCTTGATCTATCAGGATGAATTGAAACTGCCTGTTTAA
CTGTCTATCTCGATAATCCTGTAAGAATCTGAAGTTTTGCCTGAAAATGAATTTGAATTTCTTTTCGTTGTT
TTTCTTTTTGAAGAATACTTTTTGCTTTGGAA

A 4-hour time course and temperature test was performed to test the newly obtained 6 His SUMO cavin-1 construct in BL21(DE3) pLysS and to search for the optimal temperature and growth time for expression and solubility of the fusion protein. Once I determined these conditions, I would use them in subsequent purification steps to obtain protein for binding studies with caveolin-1. Two bacterial cultures were grown at 37˚C to an OD_{600} of 0.8, and induced with 0.5 mM IPTG. One culture was incubated at 29˚C and the other was incubated at 37˚C. At each time point of 1, 2, 3 and 4 hours, I collected 0.1 ml aliquots of the cultures at each temperature and prepared them for SDS-PAGE. In addition, after 3 hours of incubation, 19 ml of culture from each temperature sample were used for a solubility test to determine the relative amounts of soluble and insoluble protein present. The 19 milliliters of each culture were spun down in a refrigerated centrifuge. The resulting cell pellets were re-suspended in 400 µl Native Lysis Buffer, treated with Triton X-100 added to 1% and incubated for 45 minutes at 4˚C. The lysates were sonicated with a microtip-sonicator, and centrifuged to obtain the soluble fractions (in the supernatant) and the insoluble fractions (insoluble cell pellet).

The purified SUMO-cavin-1 was expected to have an observed molecular weight of approximately 75 kDa (55 kDa for cavin-1 and 20 kDa for the SUMO tag). The 29˚C samples on the blot showed a general pattern of increasing expression of the SUMO-cavin-1 over time, with the 4^{th}-hour time point showing the most expression at ~75 kDa. However, the level of protein expression, typified by the intensity of the signal, appeared to be lower in the 3^{rd} hour time point (lane 4 of Figure 2), compared to the 2^{nd} hour aliquot (lane 3 of Figure 2), making interpretation of the trend of expression challenging. SUMO-cavin-1 expression generally appeared to increase over time for the 37˚C samples. Peak protein expression among all the temperature samples occurred between the 3^{rd} and 4^{th} hour for the 37˚C sample (lanes 8 and 9 of Figure 2). However, the protein was mostly insoluble after induction at either 29˚C or 37˚C, with prominent bands at ~75 kDa (lanes 12 and 13 in Figure 2), compared to the faint signals observed for the total soluble fractions at each temperature (lanes 10 and 11 in Figure 2).

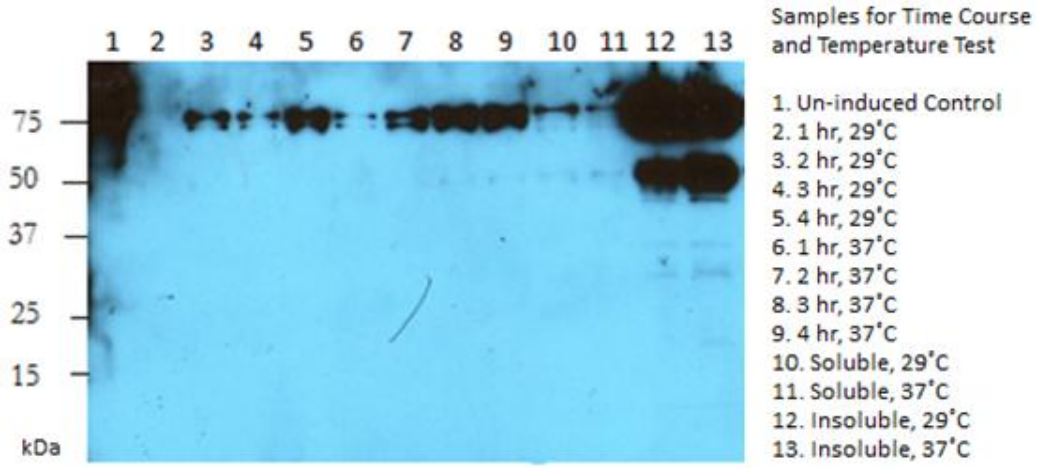

Figure 2: Four-Hour Time Course for Testing the Expression and Solubility of 6His-SUMO-cavin-1 (lab number: DB1493) for Optimal Temperature and Growth Time. DB1493 cultures were prepared as described in Materials and Methods (section 2.2), growing the cells after 0.5 mM IPTG induction at either 29°C or 37°C as indicated. Samples from each hour time point of the 4 hour time course were collected for analysis by SDS-PAGE. Cells were harvested after 3 hours of incubation to test for solubility of 6His-SUMO-cavin-1. Cell pellets were re-suspended in Native Lysis Buffer, treated with Triton X-100 to 1%, and extracted as indicated in the Methods and Materials 2.2.1. Time course and solubility test samples were analyzed by SDS-PAGE and transferred to PVDF. The blot was probed with mouse monoclonal anti-6His.

A higher quantity of soluble recombinant protein is desired in order to facilitate protein purification (Gopal and Kumar, 2013). A second solubility test (see Methods and Materials section 2.2.2) was done to observe the ratio of insoluble and soluble cavin-1 after exploring two approaches to improve solubility of the protein: testing extraction in a larger volume of lysate, while changing the sonicator model, and testing a different detergent, Fos choline-16, while using the same microtip sonicator as before. Results from previous experiments conducted by fellow lab members showed that Fos choline-16 helped solubilize cavin-1 from mammalian cells, suggesting that this detergent may stabilize the protein. For the latter approach, I wanted to compare the ability of Fos choline-16 and Triton X-100 (used in the previous experiment) to solubilize cavin-1. To test the conditions for both approaches, four-20 ml cultures were grown for 3 hours at 37˚C (based on the overall peak protein expression observed around the 3 hour mark at 37˚C in the previous experiment). The four cultures were centrifuged and approximately the same amount of cell pellet was obtained for each sample. Two cell pellets

were extracted in a large-volume of Native Lysis Buffer. The two remaining pellets were extracted as in the previous experiment and treated with either Fos choline-16 or Triton X-100. For the large-volume extraction, I re-suspended one cell pellet in 35 ml of Native Lysis Buffer, added Triton X-100 to 1%, and sonicated the lysate with the Branson 250-450 Sonifier Analog Cell Disruptor. In the previous experiment, the microtip sonicator (Branson Sonifier Cell Disruptor 185) was experiencing technical problems, and the power output was erratic. This could have led to either insufficient or excess sonication of the lysate, contributing to a higher fraction of insoluble protein. My fellow lab member repeated this large-volume extraction for the second cell pellet (lanes 2 and 3 in Figure 3). The remaining two cell pellets were re-suspended in 400 µl Native Lysis Buffer, as in the previous experiment. To compare the detergents in their ability to solubilize SUMO-tagged cavin-1, my fellow lab member added Fos choline-16 to 1% to one cell suspension, and treated the last cell suspension with Triton X-100 (TX-100) to 1% (as before). The cell lysates from these two samples were sonicated with the mictrotip sonicator, as in previous trials. All the samples, both large and small volume extractions, were centrifuged. The soluble supernatants and insoluble pellets from each sample were prepared for SDS-PAGE. The Triton X-100 and Fos choline-16 samples were loaded in duplicate lanes (samples in lanes 5-8 were duplicated in lanes 9-12 in Figure 3; equal volumes were loaded). The results of the blot are shown in Figure 3. For the large volume extraction I performed, the soluble fraction of protein showed a prominent band at ~75 kDa (lane 1 in Figure 3), while there was no strong signal in the insoluble fraction (lane 2, Figure 3) suggesting that the protein was mostly soluble. Surprisingly, for the same large-volume extraction my fellow lab member prepared in parallel, the ~75 kDa band had a stronger signal for the insoluble fraction (lane 4, Figure 3). The contrasting results may be due to the fact that the cells were extracted from two separate culture flasks. In one culture, recombinant cavin-1 may have aggregated or might have been packaged into inclusion bodies, leading to the poor solubility of the protein observed in one set of samples, while the recombinant protein may not have aggregated as much in the other culture. Thus, the results regarding extracting in a larger volume, while sonicating with a different model, are inconclusive. The soluble fractions of the Triton X-100 and Fos choline-16 samples showed little to no signal in general (lanes 5, 7, and 9

in Figure 3), while the insoluble fractions showed very strong bands at ~75 kDa. The re-loaded Fos choline-16 samples showed an exception to the trend, as there was a prominent signal in the soluble fraction (lane 11 in Figure 3). The dramatically different results of the Fos choline-16 treated sample and its duplicate run may be due to variations in sample vortexing prior to loading on the gel. If the soluble sample contents were not vortexed thoroughly when loading lane 7, there may be a lower quantity of observed soluble protein. It is also possible that some soluble supernatant remained in the centrifuge tube with the insoluble fraction, leading to the prominent signal in the insoluble sample lanes (lanes 8 and 12 in Figure 3). Possible products of proteolysis also appeared at the two bands between 37-50 kDa in lane 11. Overall, treating samples with Fos choline-16 did not appear to solubilize cavin-1.

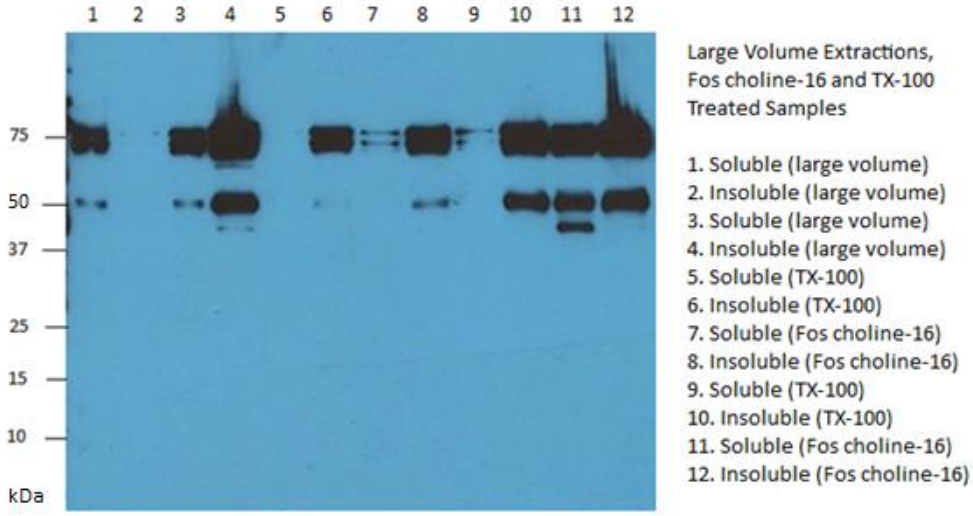

Figure 3: Testing the Solubility of 6His-SUMO-cavin-1 by Extracting Cells in a Larger Volume of Native Lysis Buffer (with a Different Sonicator) and Comparing the Solubilization of the Protein by Fos choline-16 and Triton X-100. Four cultures of DB1493 were prepared as described in Materials and Methods (section 2.2), growing the cells for 3 hours after 0.5 mM IPTG induction at 37°C. Cells were harvested after 3 hours of incubation to test for solubility of 6His-SUMO-cavin-1. Two cell pellets were re-suspended in 35 ml Native Lysis Buffer, treated with Triton X-100 to 1%, and extracted as indicated in the Methods and Materials. Lysates were sonicated with the Branson 250-450 Sonifier Analog Sonicator. The two remaining cell pellets were re-suspended in 400 µl Native Lysis Buffer, and treated with either Fos choline-16 or Triton X-100 to 1%, as indicated. Soluble and insoluble fractions of each sample were analyzed by SDS-PAGE and transferred to PVDF. Samples in lanes 5-8 were run in duplicate in lanes 9-12. The blot was probed with mouse monoclonal anti-6His.

I then tested the concurrent effects of lowering the concentration of IPTG and incubating the cultures at a lower temperature (after IPTG-induction) on the construct to determine whether these modified factors could temper the expression of cavin-1 during early incubation times, as fused cavin-1 can become toxic to the bacterial cells. At a lower temperature, such as 16˚C, peptide elongation rates are slower, as there may be a delay in translation initiation. This slower elongation rate may lead to fewer errors in protein folding. Overnight incubation of 0.1 and 0.5 mM IPTG inductions at 16˚C was also tested to compare the ratio of soluble and insoluble protein at each condition. As seen in Figure 4, expression of the protein gradually increased over time, with peak expression of SUMO-tagged cavin-1 occurring between the 3rd and 4th hour for both 0.1 mM and 0.5 mM IPTG-induced samples (lanes 2, 3, 5 and 6 in Figure 4). No band was seen for the soluble fraction for 0.1 mM IPTG-induced cells (lane 7 of Figure 4), while there was a slight band for the insoluble fraction at ~75 kDa in the adjacent lane. The overnight 0.1 mM IPTG-induced sample showed a more marked band for the insoluble fraction (lane 10 of Figure 4). While the insoluble fraction expressed more protein for the 0.5 mM IPTG-induced sample after the 3rd -hour time point, the reverse was observed for the overnight (O/N) 0.5 mM IPTG-induced samples, as the soluble fraction showed a more prominent band (lane 13 of Figure 4). Overall, the 0.5 mM IPTG-induced sample showed similar expression of protein during the time course, when compared to the sample induced with the lower IPTG concentration. Surprisingly, most soluble protein was observed at the 0.5 mM-IPTG induced overnight sample. Cells grown overnight with 0.1 mM IPTG were expected to have slower protein synthesis and more soluble protein (due to decreased protein misfolding and/or unfolding), making the observed results for the 0.5 mM IPTG overnight sample very unexpected. Because of these unanticipated results and the possibility of sample error, the 0.5 mM IPTG O/N incubation condition was not pursued in future experiments.

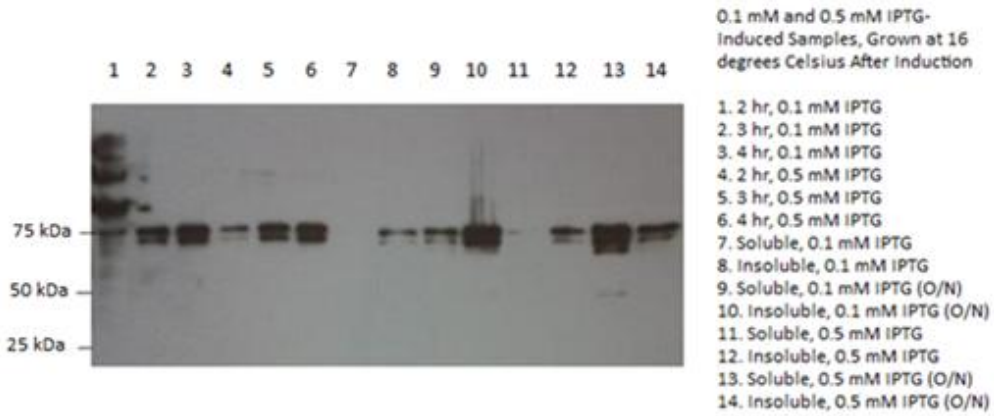

Figure 4: Test for Expression and Solubility of 6His-SUMO-cavin-1 with 0.1 mM and 0.5 mM IPTG Inductions at 16˚C. Four DB1493 cultures were prepared as described in Materials and Methods (section 2.2), growing the cells after either 0.1 mM or 0.5 mM IPTG induction at 16˚C, as indicated. Samples from each hour time point of the 4 hour time course were collected for analysis by SDS-PAGE. Cells were harvested after 3 hours of incubation to test for solubility of 6His-SUMO-cavin-1. Cell pellets were re-suspended in Native Lysis Buffer, treated with Triton X-100 to 1%, and extracted as indicated in the Methods and Materials 2.2.3 Overnight samples induced with 0.1 mM and 0.5 mM IPTG were similarly tested for solubility. Time course and all solubility test samples (including overnight samples) were analyzed by SDS-PAGE and transferred to PVDF. The blot was probed with mouse monoclonal anti-6His.

As no other growth and incubation conditions gave clear evidence of higher total expression or increased solubility of 6His-SUMO-cavin-1, I attempted to use immobilized metal affinity chromatography (IMAC) to purify 6His-SUMO-cavin-1 from the soluble extracts after cultures were induced with 0.5 mM IPTG for 3 hours at either 29°C or 37°C (as in Figure 2) by IMAC. I wanted to test these soluble extracts for binding and elution from Ni-NTA beads (designed to bind the 6His-tag). The extracts were incubated with the Ni-NTA beads for 1 hour at 4˚C, on an end-over-end rotator. After incubation, the tubes were spun in the microfuge and the unbound fraction of protein for each temperature sample was saved for SDS-PAGE. The beads were washed sequentially with HSWB at pH 8.0 containing 10 and 50 mM imidazole, before elution with 2 sequential aliquots of HSWB containing 250 mM imidazole at pH 7.0 (Methods and Materials, section 2.3.1). As shown in Figure 5 , SUMO-tagged cavin-1 was eluted during the first and second 250 mM imidazole elutions for both the 29˚C (lanes 3, and 4 in Figure 5) and 37˚C (lanes 7 and 8 in Figure 5) samples, with a more concentrated band for the latter temperature sample. Some proteolysis products could be visualized in the second 250 mM imidazole elution for the 37˚C incubated protein. For the unbound fraction for 29˚C in lane

2, bands were seen around between 75-100 kDa, but it is possible that the pre-stained protein ladder sample spread to the adjacent well, as the 37˚C unbound fraction did not exhibit any distinct bands. The results suggest the SUMO-tagged cavin-1 bound the beads well, and could be eluted from the resin.

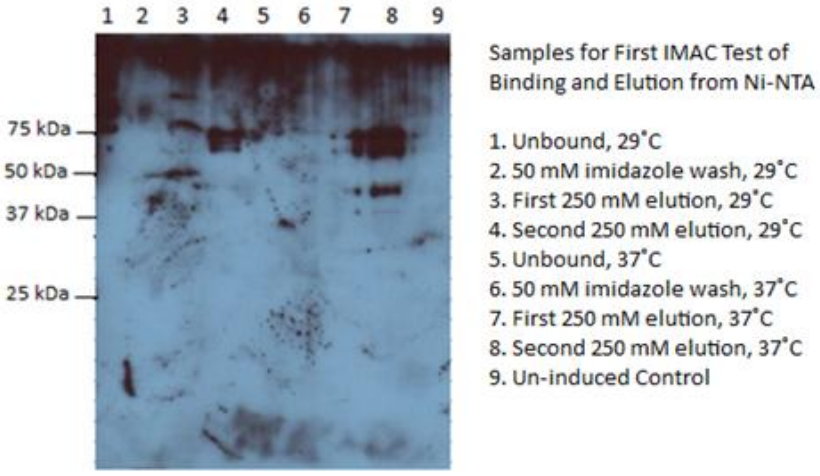

Figure 5: Testing the Binding and Elution of SUMO-tagged cavin-1 from Ni-NTA beads. 6His-SUMO-cavin-1 was expressed in E. coli BL21(DE3) as described in Materials and Methods growing the cells after IPTG induction at either 29°C or 37°C as indicated. Cells were lysed and subjected to IMAC as described in Materials and Methods. Samples of the unbound cell lysate after bead binding, the 50 mM imidazole wash, and the first and second 250 mM imidazole eluates from each sample were analyzed by SDS-PAGE and transferred to PVDF. The blot was probed with mouse monoclonal anti-6His.

As previous work in the lab had shown that Fos choline-16 helped solubilize cavin-1 from mammalian cells, I wanted to explore whether including Fos choline-16 in the IMAC wash and elution solutions could also facilitate the elution of 6His-SUMO-cavin-1 from the Ni-NTA resin, possibly by limiting unfolding of the protein, or accumulation of aggregates that might inhibit release from the beads. I tested a revised IMAC procedure on all the soluble extracts from samples collected after 3 hours of incubation after induction and overnight samples, all grown at the 16˚C after induction with 0.1/0.5 mM IPTG. I adjusted all the prepared wash and elution buffers (WB-10, WB-50 and EB-250) with a final concentration of 0.00053% of Fos choline-16, which is 2.5 times the critical micelle concentration (CMC). The high salt wash buffers (HSWB)

and imidazole solution used in this experiment did not contain any Triton X-100. Beads with bound protein were washed with HSWB pH 8.0 containing 10 mM imidazole (WB-10). The third wash supernatant was saved for SDS-PAGE (sample in lane 3 of Figures 6a and 6b). The Ni-NTA resin for each sample was washed twice with HSWB pH 8.0 containing 50 mM imidazole (WB-50-1 and WB-50-2). Two sequential elutions were performed with HSWB pH 7.0 containing 250 mM imidazole (EB-250-1 and EB-250-2). One gel contained both the 0.1 mM IPTG-induced 3rd hour and overnight samples grown at 16˚C (Figure 6a), while another gel was run for the 0.5 mM overnight samples grown at 16˚C (Figure 6b). The gel in Figure 6b was loaded with 5 and 15 µl of 1:100 dilutions of each sample. A band at ~75 kDa was seen in both the unbound and soluble fractions of the overnight 0.1 mM IPTG-induced sample (lanes 8 and 9, respectively, in Figure 6a). The signal seen for the unbound protein suggests that the recombinant protein did not bind well to the bead resin. Possible bands for the protein were also seen for the soluble and unbound fractions for the 3rd hr samples (lanes 1 and 2 of Figure 6a), but they may be from a dark protein ladder signal covering those lanes. In the Western blot for the 0.5 mM IPTG-induced overnight samples, a band at ~75 kDa was observed for the soluble fraction of protein for the 15 µl loaded of a 1:100 dilution (lane 8 of Figure 6b). SUMO-tagged cavin-1 did not appear in any of the washes nor for any elutions in Figure 6b. Overall, while soluble SUMO-cavin-1 could be detected, the recombinant protein could not be eluted off the Ni-NTA beads for both 0.1 and 0.5 mM samples. Approaches for enhancing release of protein from the resin needed to be tested in the next experiment.

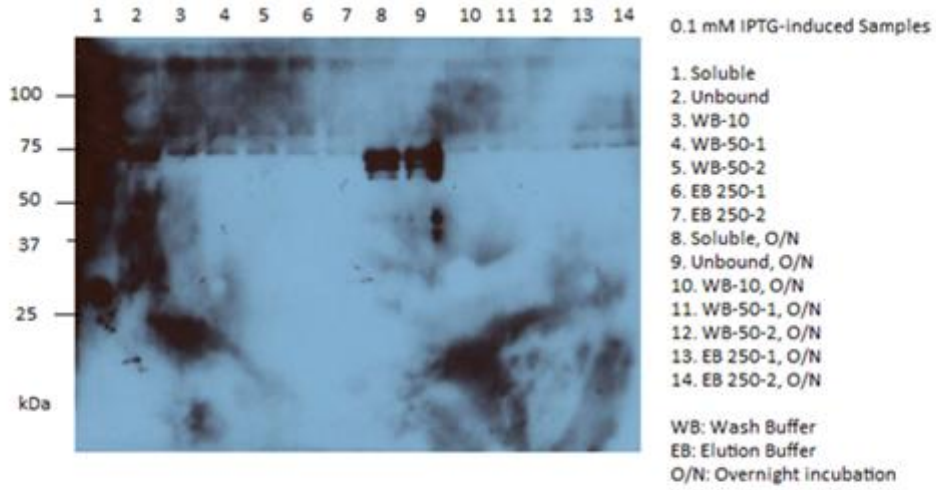

Figure 6a: IMAC Binding Test for 0.1 mM IPTG-induced Samples, Substituting Fos choline-16 (0.00053%) for Triton X-100 in Washes and Elutions. Cultures were induced with 0.1 mM IPTG, and grown at 16˚C, either for 3 hours or overnight, as indicated. Cells were lysed and subjected to IMAC with 0.00053% Fos choline-16-supplemented washes and elutions (as in Methods and Materials, section 2.3.2). Samples of the soluble fraction , unbound cell lysate after bead binding, the 10 mM imidazole wash, the two 50 mM imidazole washes, and the two 250 mM imidazole elution fractions were analyzed by SDS-PAGE and transferred to PVDF. The blot was probed with anti-6His.

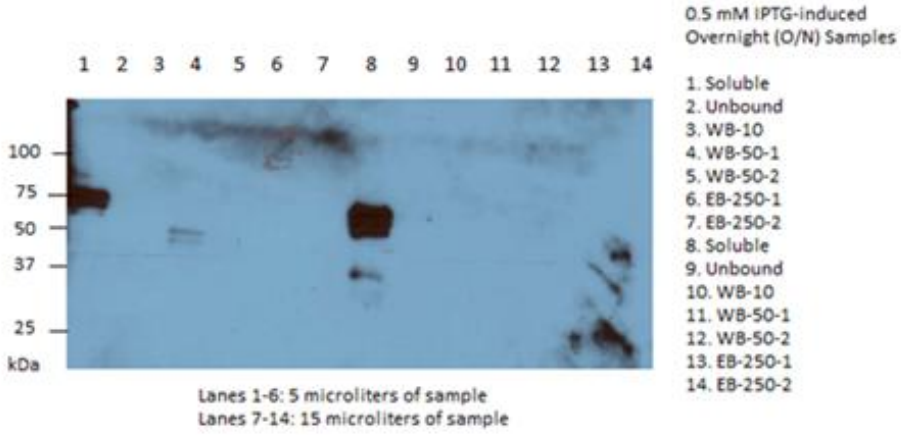

Figure 6b: IMAC Binding Test for 0.5 mM IPTG-induced Samples, Substituting Fos choline-16 (0.00053%) for Triton X-100 in Washes and Elutions. Cultures were induced with 0.5 mM IPTG, and grown at 16˚C, overnight. IMAC was performed as in 2.3.2. Samples of the soluble fraction, unbound cell lysate after bead binding, the 10 mM imidazole wash, the two 50 mM imidazole washes, and the two 250 mM imidazole elution fractions were analyzed by SDS-PAGE and transferred to PVDF. The blot was probed with anti-6His.

In the next IMAC procedure, I tested a higher concentration of Fos choline-16 at 0.1%, and also explored using N-lauroyl sarcosine, in the final elution solutions. The detergent, N-lauroyl sarcosine, can aid solubilization of foreign eukaryotic proteins expressed in bacterial hosts which may be packaged into inclusion bodies (Tao et al, 2010). In earlier experiments by other lab members, N-lauroyl sarcosine aided the release of GST-cavin-1 from glutathione beads. I wanted to assess this detergent's ability to release 6His-SUMO-cavin-1 from Ni-NTA resin. During the cell culture setup, the OD_{600} , prior to induction with 0.5 mM IPTG, accidentally reached 1.46, instead of the desired 0.8. The higher optical density may have altered the pH of the cell lysate, affecting the binding capacity and/or specificity to the Ni-NTA beads. The bacterial cells were pelleted after 4 hours of incubation after induction with 0.5 mM IPTG. When the cell pellet was re-suspended in Native Lysis Buffer (supplemented with lysozyme and Fos choline-16) during the extraction, the lysate was much more viscous than lysates in previous experiments. This led to some loss of sample during transfers between tubes. The higher cell density and possible release of DNA after lysing may have contributed to the thicker consistency. I treated the sample containing lysate and Ni-NTA beads with the wash and elution buffers, WB10, WB50-1, WB50-2 and EB250-1, prepared as before. The final two elutions, were done with an N-lauroyl sarcosine-supplemented elution buffer containing a final concentration of 0.1% N-lauroyl sarcosine. This was prepared like EB-250, except N-lauroyl sarcosine was added to the elution buffer to a final concentration of 0.1% from a stock solution of 1% N-lauroyl sarcosine in 50 mM Tris, pH 8.0. No visible protein bands were seen for the insoluble fraction of the protein, while a prominent band at ~75 kDa appeared in the soluble fraction (lane 2 of Figure 7). However, most of the protein did not bind to the Ni-NTA beads, as the unbound fraction showed a strong signal at 75 kDa (lane 3 of Figure 7) with similar intensity as that of the soluble fraction. No 6His- SUMO-cavin-1 was eluted from the beads when the 250 mM imidazole elution buffer contained N-lauroyl sarcosine. Whether the increased optical density of the bacterial cultures influenced binding and elution outcomes needed to be examined in the following experiment.

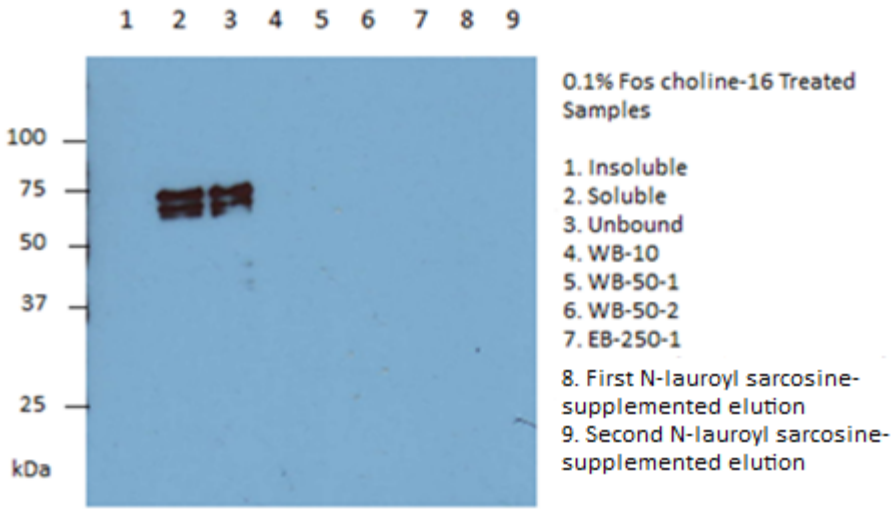

Figure 7: Second Test of Binding and Release of 6His-SUMO-cavin-1 from Ni-NTA Beads Blot Using an Increased Fos choline-16 Concentration (0.1%) in Washes/Elutions and 0.1% N-lauroyl sarcosine-supplemented Elutions. Cells were lysed and subjected to IMAC with 0.1% Fos choline-16-supplemented washes /elutions and final imidazole elutions supplemented with 0.1% N-lauroyl sarcosine (as in Methods and Materials, section 2.3.3). Samples of the insoluble pellet, soluble fraction , unbound cell lysate after bead binding, the 10 mM imidazole wash, the two 50 mM imidazole washes, the first 250 mM imidazole eluate and final two N-lauroyl sarcosine-supplemented 250 mM imidazole eluates were analyzed by SDS-PAGE and transferred to PVDF. The blot was probed with anti-6His.

I repeated the previous experiment and induced the cells with 0.5 mM IPTG when the OD_{600} was closer to the desired 0.80 value, at 0.81. The final Fos choline-16 concentration, 0.1%, was maintained in the wash and elution buffers. A large insoluble pellet was obtained after the extraction procedure. The erratic power output of the microtip sonicator used in the experiment or incomplete lysing of the cells may have caused this. There was a more prominent band at ~75 kDa for the insoluble protein (lane 1 of Figure 8) compared to the band for soluble protein. The 6 His SUMO-cavin-1 did not bind well to the bead matrix, as shown by the bands in the unbound fraction (lane 3 of Figure 8). N-lauroyl sarcosine did not elute 6His-SUMO-cavin-1 off the Ni-NTA beads.

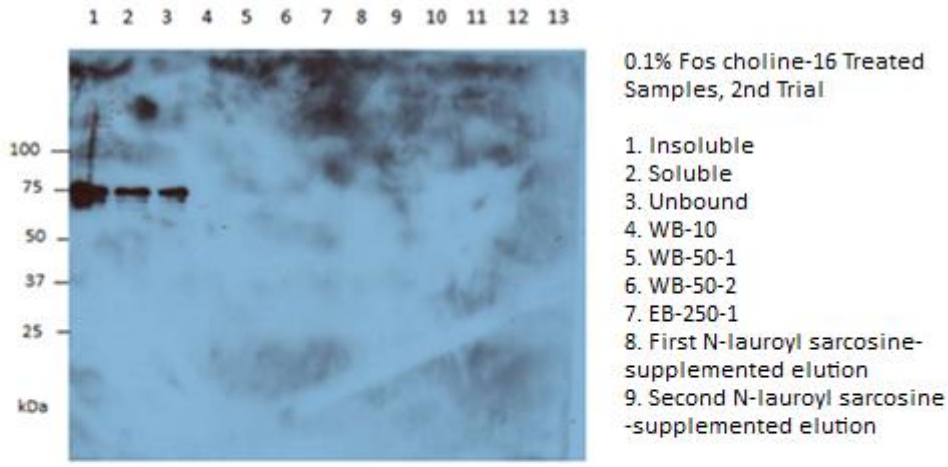

Figure 8: Second Test of Binding and Release of 6His-SUMO-cavin-1 from Ni-NTA Beads Blot Using an Increased Fos choline-16 Concentration (0.1%) in Washes/Elutions and 0.1% N-lauroyl sarcosine-supplemented Elutions. Cultures were grown to OD600= 0.81, close to the desired density of 0.8. Cells were lysed and subjected to IMAC with 0.1% Fos choline-16-supplemented washes /elutions and final imidazole elutions supplemented with 0.1% N-lauroyl sarcosine(as in Methods and Materials, section 2.3.3). Samples of the insoluble pellet, soluble fraction , unbound cell lysate after bead binding, the 10 mM imidazole wash, the two 50 mM imidazole washes, the first 250 mM imidazole eluate and final two N-lauroyl sarcosine-supplemented 250 mM imidazole eluates were analyzed by SDS-PAGE and transferred to PVDF. The blot was probed with anti-6His.

Cavin-1 may oligomerize when expressed in bacterial hosts, resulting in complexes which may bind the nickel beads with very high avidity. As a result, the final 250 mM imidazole elutions may not have released the proteins from the resin with high efficiency. Since EDTA can chelate nickel from the beads, I conducted a new IMAC experiment to test a final EDTA elution of SUMO-cavin-1 to assess its ability to release the protein. The imidazole solutions used for the wash and elution solutions in IMAC had some precipitate at the bottom of the tube, so in this experiment, I made sure to warm up the solution in a water bath and vortex thoroughly to dissolve any remaining crystals. This extra precaution was not taken in the previous experiments, and may have led to the poor elution results. The cavin-1 was mostly soluble, as shown by the prominent band at ~75 kDa in the total soluble fraction (lane 2 in Figure 9). Some proteolytic cleavage products could also be seen in that lane. Some of the protein still showed up in the unbound fraction (lane 3 in Figure 9), and possible products from proteolysis were seen as well. These extraneous products were not observed in the first 50 mM imidazole wash

sample. Some 6His-SUMO-cavin-1 was eluted with 50 mM imidazole, but at a lower intensity compared to that of the unbound protein. No 6His-SUMO-cavin-1 was eluted by EDTA. This showed that the poor elution of cavin-1 from Ni-NTA beads was not caused by high-avidity binding of oligomerized cavin-1 to the beads. It is possible that cavin-1 bound the beads non-specifically.

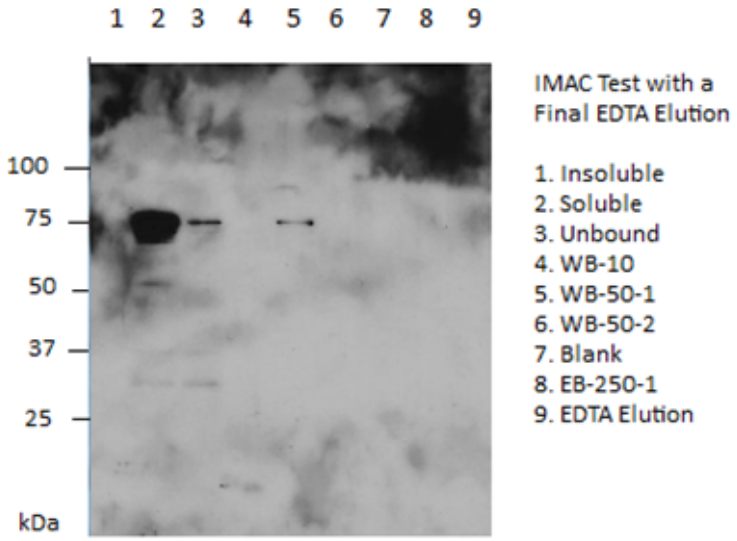

Figure 9: Testing Elution with EDTA to Release Protein from Ni-NTA Beads. Cells were lysed and subjected to IMAC with 0.1% Fos choline-16-supplemented washes /elutions. A final elution was performed using elution buffer containing EDTA (see Methods and Materials, section 2.3.4). Samples of the insoluble pellet, soluble fraction, unbound cell lysate after bead binding, the 10 mM imidazole wash, the two 50 mM imidazole washes, the first 250 mM imidazole eluate and final EDTA elution were analyzed by SDS-PAGE and transferred to PVDF. The blot was probed with anti-6His.

Despite testing several different parameters, we could not successfully obtain sufficient quantities of 6His-SUMO-cavin-1 by IMAC. Low solubility of the recombinant protein, poor release and inefficient binding to the Ni-NTA resin appeared to be the biggest contributors to low yield. The GST-cavin-1 construct (lab number: DB1298) was successfully expressed in BL21 (DE3) in earlier experiments. While tests on the GST-cavin-1 construct showed acceptable levels of solubility, bead binding affinity and elution of the protein, the results were not optimal, prompting the initial trials on the 6His-SUMO-cavin-1 fusion protein. However, as the studies on

6His-SUMO-cavin-1 did not produce desirable results, I revisited the GST-cavin-1 construct for protein purification.

I first tested expression and solubility of GST-cavin-1, as well as binding to and release from glutathione beads, using conditions established earlier in the lab. BL21 (DE3) bacteria transformed with the GST-cavin-1 construct were induced with 0.5 mM IPTG for 4 hours at 37°C before subsequent lysed with Native Lysis Buffer and treated with 1% Triton X-100. The cell lysate was incubated with glutathione-agarose beads for 2 hours at 4°C (Methods and Materials, section 2.4.1). The unbound protein fraction was saved for SDS-PAGE. The beads containing bound protein were rinsed 3 times with Native Lysis Buffer and the wash supernatants were discarded. The beads were incubated at room temperature for 20 minutes with glutathione-elution buffer containing 50 mM Tris (pH 8.0), 10 mM reduced glutathione and 0.1% N-lauroyl sarcosine. To determine how much protein remained on the glutathione-agarose beads after elution, I rinsed the beads once with 50 mM Tris pH 8.0, pelleted them and re-suspended the pellet in 2X SDS-SB for SDS-PAGE (SDS- beads sample). Purified GST-cavin-1 was predicted to have an observed molecular weight of ~75 kDa (55 kDa from the cavin-1 and ~20 kDa for the GST tag).The results from Figure 10 showed GST-cavin-1 release from the glutathione-agarose beads, as exhibited by the ~75 kDa band seen in lane 3, but there was still a significant fraction of unbound protein (lane 2 of Figure 10). I performed a second test on the GST-cavin-1 construct by repeating the aforementioned cell lysis, incubation and bead wash steps, but I tested a slightly longer glutathione-elution by incubating the beads with the elution buffer for a total of 30 minutes (instead of 20 minutes, as in the previous experiment). The results were similar to those in Figure 10 (data not shown). There is still a considerable fraction of the protein that did not bind to the resin. These sets of results do resemble the trends observed in Coomassie gels from earlier experiments testing GST-cavin-1 release from the glutathione-agarose beads. Previous Coomassie gels showed significant noise in the soluble and unbound fractions, while the glutathione-eluted and SDS-beads samples exhibited expression of the protein in approximately similar quantities. As observed in both these experiments, while the GST-cavin-1 shows some degree of bead-binding, the quantity of unbound protein exceeds the amount of released GST-cavin-1. Techniques to enhance binding to the glutathione-agarose

beads, and recover any residual GST-cavin-1 from the unbound protein fraction needed to be explored.

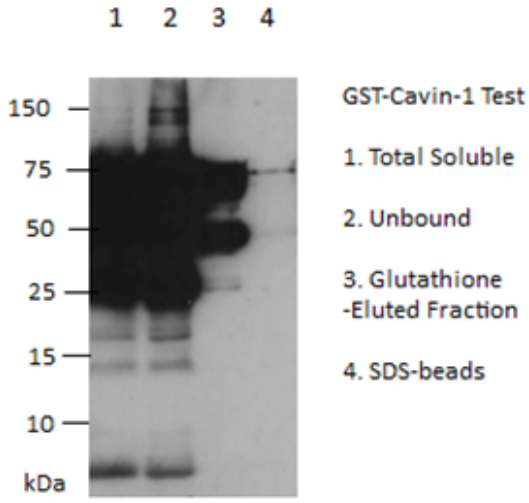

Figure 10: Testing the GST-cavin-1 Construct (DB1298) for Expression, Solubility and Binding/Release from Glutathione-Agarose Beads. A culture of DB1298 was induced with 0.5 mM IPTG and grown at 37˚C for 4 hours. After 4 hours of incubation, cells were subjected to lysis and binding with glutathione-agarose beads according to Methods and Materials, sections 2.4 and 2.4.1. The beads containing bound protein were eluted with glutathione-elution buffer, prepared as in 2.4.1. The remaining bead pellet was lysed with 2x SDS-SB (SDS-beads sample). Samples of the total soluble fraction, unbound cell lysate after bead binding, the glutathione-eluted fraction and the SDS-lysed beads were analyzed by SDS-PAGE and transferred to PVDF. The blot was probed with polyclonal rabbit anti-PTRF.

Since much of the GST-cavin-1 remained in the unbound fraction in the previous two experiments, this reduced the possible yield of purified protein. I wanted to increase the GST-cavin-1 yield from the previous experiment, so I re-incubated the unbound fraction of protein with the glutathione-agarose beads and eluted the sample with glutathione to test if some protein could be salvaged. In this new experiment, I also tested two other approaches to enhance binding to the beads (Methods and Materials, section 2.4.2). Two cultures of DB1298 were prepared. For one cell culture, the IPTG-induction conditions were the same as used in the previous experiment. With this sample, I tested the unlikely possibility that GST-cavin-1 had saturated the binding sites on the beads in the previous experiment by using thrice (3X-beads) the concentration of glutathione-agarose in the bead-binding step. For the second culture, I induced the BL21 (DE3) cells with 0.5 mM IPTG at 16˚C to see if any protein folding issues could

be resolved. If cavin-1 unfolded or misfolded during induction, the protein might not have been able to efficiently bind the beads. The re-incubated unbound, 3X beads and 16˚C samples were run in parallel for SDS-PAGE and the results from the blot are shown in Figure 11. The soluble and unbound fractions of both the 16˚C and 3X-beads samples show faint bands at ~75 kDa (lanes 1, 2, 5, and 6 of Figure 11). The unbound fraction from the re-incubated unbound sample showed bands at ~75 kDa as well (lane 9 of Figure 11). No GST-cavin-1 could be salvaged from the re-incubated unbound sample. New methods to aid binding and release of GST-cavin-1 from the glutathione-agarose beads needed to be investigated.

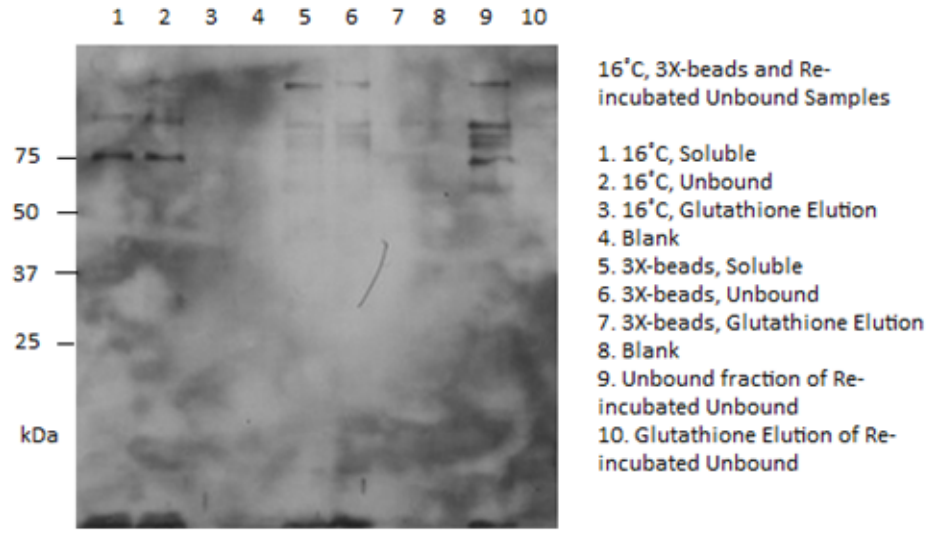

Figure 11: Testing Binding, Release and Recovery of GST-cavin-1 with a 16˚C Incubation, Increased Bead Volume (3X-beads), and Re-incubation of the Unbound Fraction (from 2.4.1). Two new cultures for the 16˚C and the 3X-beads samples were grown for 4 hours and induced as in Methods and Materials, section 2.4.2. Cells from these two cultures were subjected to lysis and binding with glutathione-agarose beads. The 3X-beads sample was incubated with three times the previous volume of beads. The unbound protein from the previous experiment was re-incubated with the glutathione-agarose beads to test for binding and recovery of residual GST-cavin-1. The soluble fractions, unbound proteins, and glutathione-elutions for the 16˚C, 3X-beads and re-incubated unbound samples were analyzed by SDS-PAGE and transferred to PVDF. The blot was probed with polyclonal rabbit anti-PTRF.

My tests on the GST-cavin-1 construct were performed with BL21 (DE3) cultures grown at 37˚C for 4 hours after induction. In my next experiment, I tested a 2-hour incubation of the bacterial culture at 29˚C, after induction with 0.5 mM IPTG, as earlier work in the lab under these experimental conditions showed promising release of GST-cavin-1. The total soluble and unbound fractions of the protein exhibited a similar pattern of a series of bands, including

bands near the 75 kDa mark (lanes 1 and 2 of Figure 12). Although the issue of lack of inefficient bead-binding remained, GST-cavin-1 was successfully eluted (lane 4 of Figure 12) and not much protein remained on the beads after glutathione elution (lane 5 of Figure 12). These results suggest inefficient initial binding of the protein, but efficient release by glutathione of the small amount of GST-cavin-1 that bound to the beads. Improving GST-cavin-1 solubilization could enhance bead binding. The detergent, Triton X-100, was added to cell extracts in GST-cavin-1 experiments. The ability of an alternate detergent, Fos choline-16, to solubilize GST-cavin-1 would be tested in the following experiment.

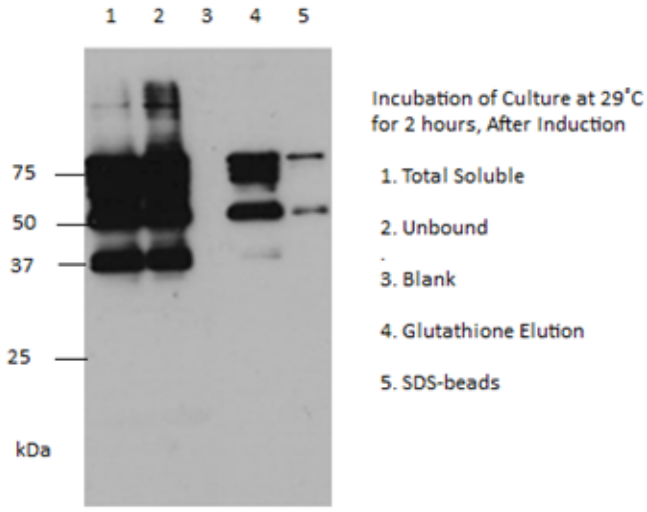

Figure 12: Testing Binding and Release of GST-cavin-1 After a Combined 29˚C and 2 -hour Incubation. A culture was induced with 0.5 mM IPTG, and incubated for 2 hours at 29˚C. Cells were subjected to lysis and binding with glutathione-agarose beads according to Methods and Materials, sections 2.4 and 2.4.1. The beads containing bound protein were eluted with glutathione-elution buffer, prepared as in 2.4.1. The remaining bead pellet was lysed with 2x SDS-SB (SDS-beads sample). Samples of the total soluble fraction, unbound cell lysate after bead binding, the glutathione-eluted fraction and the SDS-lysed beads were analyzed by SDS-PAGE and transferred to PVDF. The blot was probed with polyclonal rabbit anti-PTRF.

I then compared the effects of treating cell lysates with Fos choline-16 or Triton X-100 on GST-cavin-1 solubilization after incubating 0.5 mM IPTG induced cultures for 2 hours at 29˚C. The two detergents showed similar band patterns and intensity for the total soluble and unbound fractions of the protein. The issue of the high proportion of unbound protein still

persisted. The glutathione-elutions for both detergents exhibited a strong signal at the ~75 kDa mark, suggesting GST-cavin-1 was successfully eluted from the beads (lanes 4 and 10 in Figure 13). The insoluble fraction of the protein showed a very low signal for the sample treated with Triton X-100, while strong bands at 75 kDa and below were observed for the insoluble fractions for Fos choline-16 treated samples. It is possible that Triton X-100 facilitates the solubilization of the protein better than Fos choline-16 does. However, the prominent signal seen in the insoluble fraction for the Fos choline-16-treated sample (lane 7 of Figure 13) may be due to the presence of some soluble supernatant in the insoluble pellet. As the insoluble cell pellet for this sample was small, it was difficult to completely remove the soluble supernatant without disturbing the pellet. While there appears to be no significant difference between the detergents for the amount of GST-cavin-1 eluted, the results suggest that the Triton X-100 treated sample released GST-cavin-1 from the beads better, as less protein is seen in the SDS-beads fraction (lane 5 of Figure 13) compared to the SDS-beads sample for Fos choline-16 (lane 11 of Figure 13).

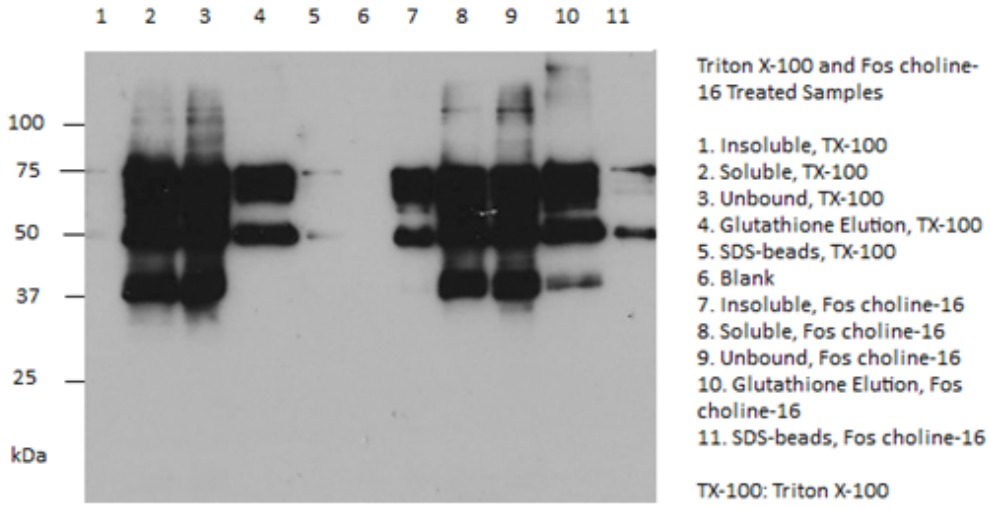

Figure 13: Comparing Solubilization of GST-cavin-1 with Different Detergents, Triton X-100 and Fos Choline-16. Two cultures were induced with 0.5 mM IPTG, and incubated for 2 hours at 29˚C. Cells from one culture were extracted and treated with Fos choline-16 to 1%. Cells from the other culture were extracted and treated with Triton X-100, as before. Binding and incubation with glutathione-agarose beads were done according to Methods and Materials, section 2.4.4. The beads containing bound protein were eluted with 600 µl glutathione-elution buffer, prepared as in 2.4.1.The remaining bead pellets were lysed with 2x SDS-SB (SDS-beads sample). Samples of the total soluble fraction, unbound cell lysate after bead binding, the glutathione-eluted fraction and the SDS-lysed beads for both detergent treatments were analyzed by SDS-PAGE and transferred to PVDF. The blot was probed with polyclonal rabbit anti-PTRF.

Because the results from the tests on GST-cavin-1 suggested that I might be able to obtain enough GST-cavin-1 for our binding studies, I performed a larger-scale, 2 liter preparation of GST-cavin-1. The 0.5 mM IPTG-induced cultures were grown for 3 hours, at 37˚C. Cells were lysed, and incubated with glutathione-agarose beads as in Methods and Materials, section 2.4.5. The results of the Western Blot suggest a high quantity of GST-cavin-1 still remained insoluble. However, GST-cavin-1 was also detected in the cleared lysate (lane 2 of Figure 14). A similar band pattern was observed for the unbound fraction, suggesting inadequate saturation of bead binding sites. However, the glutathione-elution sample exhibits a discrete set of bands around ~75 kDa (lane 4 in Figure 14), suggesting successful preparation of GST-cavin-1. The glutathione-eluted protein also exhibits fewer extraneous bands, suggesting that there may be fewer impurities or proteolytic cleavage products in the purified sample. A comparable amount of GST-cavin-1 was observed in the SDS-SB beads sample (lane 5 of Figure 14), suggesting that some of the purified protein was still bound to the resin after glutathione elution.

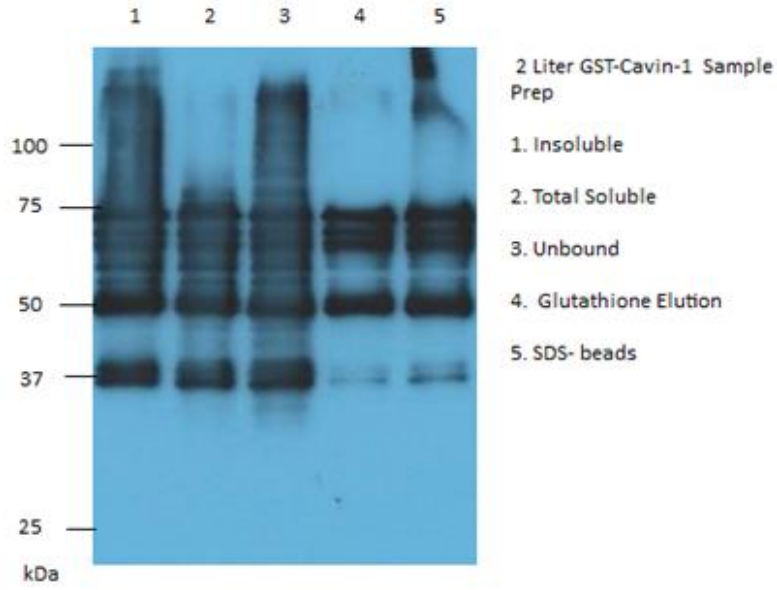

Figure 14: Test of Binding and Release of GST-cavin-1 for a 2-liter preparation. A 2 liter culture of GST-cavin-1 in BL21 (DE3) was prepared, cells were lysed, and bead binding/elutions were performed according to Methods and Materials, section 2.4.5. Samples of the total soluble fraction, unbound cell lysate after bead binding, the glutathione-eluted fraction and the SDS-lysed beads were analyzed by SDS-PAGE and transferred to PVDF. The blot was probed with polyclonal rabbit anti-PTRF.

I prepared a Coomassie gel (Figure 15) for the 2 liter culture of GST-cavin-1, and loaded it with bovine serum albumin (BSA) standards, ranging from 0.2 to 2 µg. Based on the BSA

standard curve, it was determined that 10 µl of glutathione eluate contained approximately 0.1 to 0.2 µg of protein. In a total of 1.5 ml eluate, 30-60 µg of cavin-1 were estimated to be present in the sample, and the protein concentration was approximated to be 30 µg/ml.

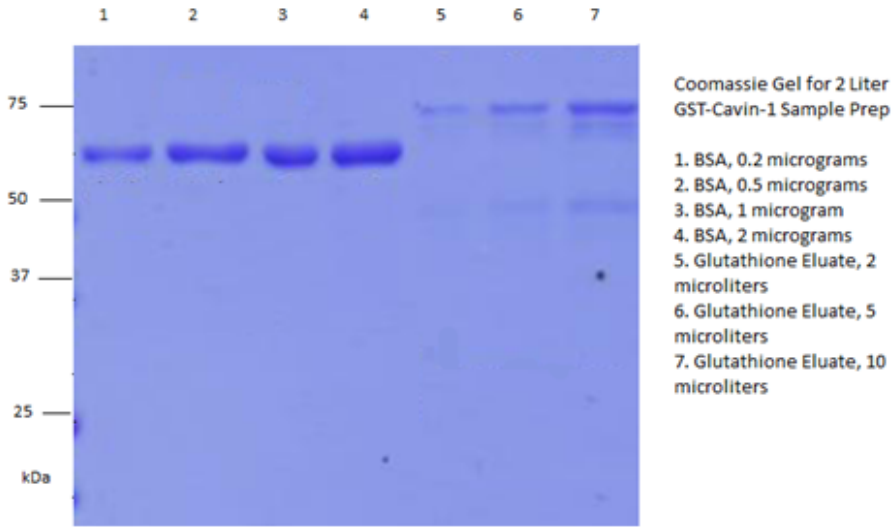

Figure 15: Coomassie Gel for 2 liter GST-cavin-1 preparation. BSA standards from 0.2-2 micrograms were loaded on an SDS-PAGE gel. Three volumes of Glutathione-eluate from the 2-liter GST-cavin-1 preparation were loaded on the same gel. The gel was stained with Coomassie blue and de-stained overnight with 30% methanol and 10% acetic acid.

The main objective of this study was to obtain sufficient quantities of purified, full-length cavin-1 for binding studies with caveolin-1. As GST-cavin-1 was successfully obtained from the 2-liter preparation, I performed a preliminary diagnostic experiment to check for possible binding to 6His-caveolin-1 on Ni-NTA beads. In an earlier experiment in the lab, 6-His-caveolin-1 was expressed in mammalian cells (HEK-293) and successfully purified by IMAC (Figure 16).

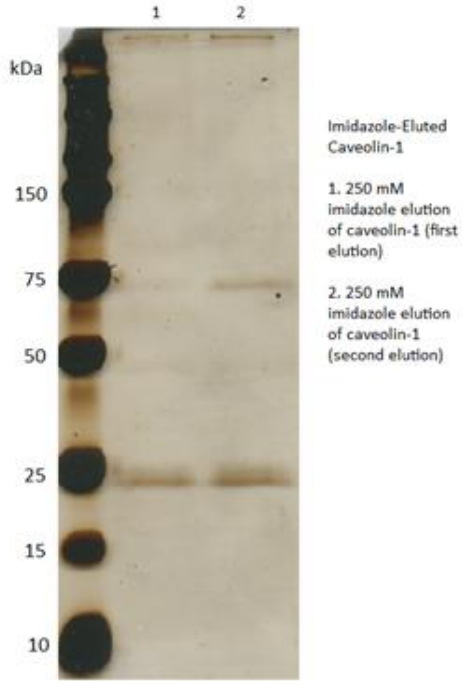

Figure 16: Purification of 6His-caveolin-1 by IMAC (Performed by Anne Ostermeyer-Fay). The 6His-caveolin-1 was expressed in mammalian cells, HEK-293. The two sample lanes in this silver-stained gel contain the 2 sequential elutions with 250 mM imidazole. Caveolin-1 protein is ~25 kDa. This protein appears at ~25 kDa for both imidazole elutions. The second elution with 250 mM imidazole (lane 2) was selected for the cavin-1 and caveolin-1 binding experiment.

Two aliquots of Ni-NTA beads were prepared for this experiment: one control sample containing only GST-cavin-1 and one experimental sample containing both 6His-caveolin-1 and GST-cavin-1. The 6His-caveolin-1 sample was diluted to contain 10 mM imidazole, allowing the protein to re-bind the Ni-NTA beads. The control sample was expected to show no binding, as it contained only GST-cavin-1 and could not bind specifically to the Ni-NTA beads. The experimental sample was designed to test for an interaction between caveolin-1 and cavin-1. If this interaction occurred, GST-cavin-1 would associate indirectly with the Ni-NTA beads through 6His-caveolin-1, which should bind the beads directly via the 6His-tag (anchoring the caveolin-1 and cavin-1 complex, if it formed). The predicted model of interaction is shown in Figure 17.

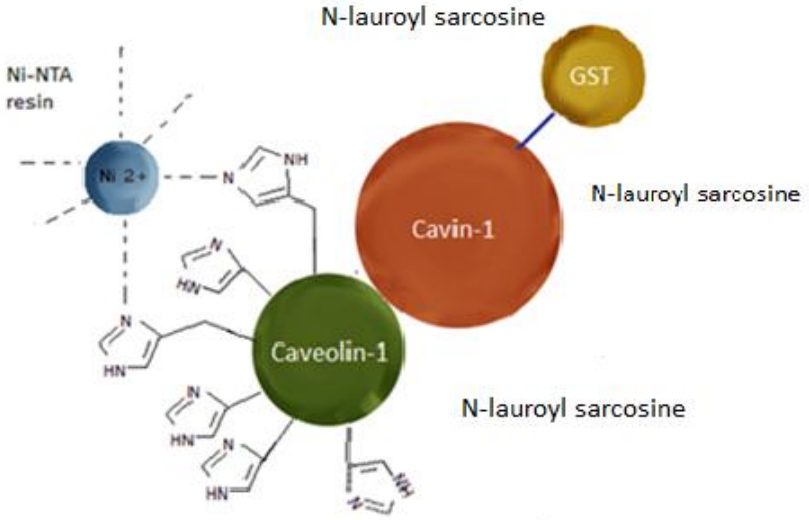

Figure 17: Possible schematic of caveolin-1 and cavin-1 interaction. The caveolin-1 will be anchored to the Ni-NTA resin through its 6His-fusion tag. The stoichiometry of the association is not well-characterized. N-lauroyl sarcosine buffer will be in the local environment of the possible cavin-1 and caveolin-1 complex.

To the control Ni-NTA beads, I added ~ 10.5 µg GST-cavin-1 (from the 2-liter preparation), Ni-NTA elution buffer (defined as TBS, pH 7.0, 200 mM NaCl and 250 mM imidazole) and TBS (20 mM Tris and 200 mM NaCl, pH 7.0). The experimental sample was prepared with ~ 2.5 µg caveolin-1, ~ 10.5 µg cavin-1 and TBS. Both samples were supplemented with a final concentration of 0.00053% Fos choline-16 and 0.1% N-lauroyl sarcosine. I incubated the samples for 2 hours at room temperature, and collected the unbound fractions for SDS-PAGE. The bead pellets with bound protein were rinsed with TBS and incubated for 10 minutes at room temperature with Ni-NTA elution buffer containing 0.00053% Fos choline-16 and 0.1% N-lauroyl sarcosine. The imidazole-eluted fractions were collected for SDS-PAGE. One PVDF membrane from the Western blot transfer was probed with anti-caveolin-1 and the other blot was probed with anti-PTRF.

The blot shown in Figure 18a was probed with anti-caveolin-1 primary antibody. The observed molecular weight of caveolin-1 is approximately 22-25 kDa. A prominent band at ~25 kDa in lane 1 in Figure 18a confirms the presence of purified caveolin-1 in the starting material.

As expected, the lane containing only GST-cavin-1 incubated with Ni-NTA beads did not show any bands in the blot, as the primary antibody did not target this protein. Lane 3 of Figure 18a contained the imidazole-eluted fraction of the cavin-1 and caveolin-1 combined sample incubated with the Ni-NTA resin. A bold band at ~25 kDa confirmed the presence of caveolin-1 and showed that 6His-caveolin-1 successfully re-bound the Ni-NTA beads in this experiment. This finding is very significant; if caveolin-1 was not detected in this lane (due to lack of binding with the Ni-NTA), cavin-1 would not show up in the anti-PTRF probed blot in Figure 18b, even if it did bind caveolin-1. Binding of 6His-caveolin-1 to the beads is necessary for testing whether cavin-1 can also bind indirectly to the resin. Without 6His-caveolin-1 anchored to the Ni-NTA resin, any associated cavin-1 would be undetected in an anti-PTRF probed blot.

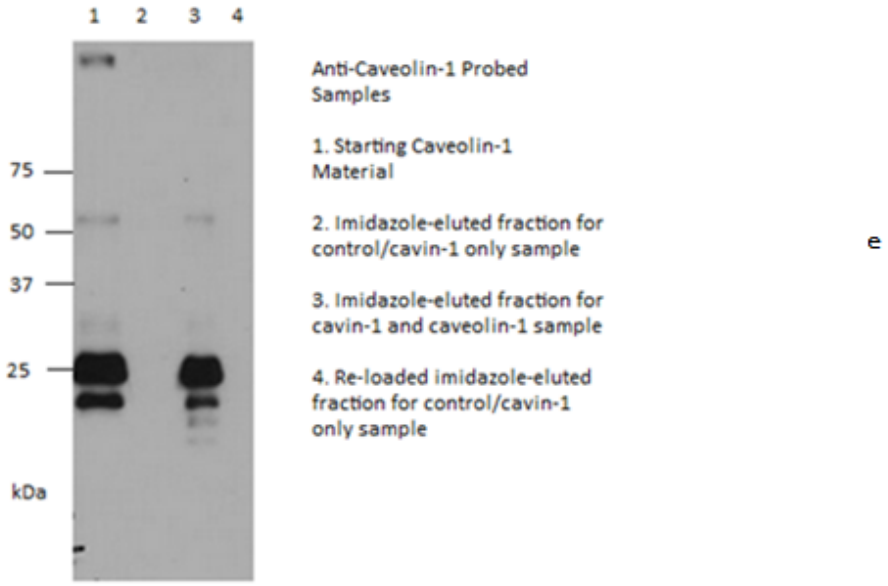

Figure 18a: Test for Binding of 6His-caveolin-1 to Ni-NTA Beads in the Cavin-1 and Caveolin-1 Binding Experiment. Samples were prepared on washed Ni-NTA beads, as described in Methods and Materials, section 2.5. The experimental samples contained cavin-1 and caveolin-1, while the control sample contained only cavin-1. The Ni-NTA bead pellets with bound protein were rinsed with TBS and incubated for 10 minutes at room temperature with Ni-NTA elution buffer containing 0.00053% Fos choline-16 and 0.1% N-lauroyl sarcosine. The imidazole-eluted fractions were collected for SDS-PAGE and transferred to a PVDF membrane. The blot was probed with anti-caveolin-1.

The other blot (Figure 18b) was probed with anti-PTRF primary antibody to determine whether GST-cavin-1 bound 6His-caveolin-1. The cavin-1 starting material was confirmed to contain GST-cavin-1, as detected by the band at ~75 kDa in lanes 1 and 2 of Figure 18b. A protein of ~50 kDa was seen in all eluted fractions for both control (incubated with GST-cavin-1 only) and experimental (incubated with 6His-caveolin-1 and GST-cavin-1) samples. The same amount of protein was eluted from beads in both samples. This suggests that the ~50 kDa band might correspond to a background that bound non-specifically to the resin.

Cavin-1 was not eluted from the beads in the experimental samples containing cavin-1 and caveolin-1, as no band at ~75 kDa (corresponding to GST-cavin-1) appeared in the blot for lanes 4 and 7 of Figure 18b. As no cavin-1 was detected in the eluate, an indirect association (via an interaction with 6His-caveolin-1) with the resin could not be determined. Thus, these results showed no detectable binding association between caveolin-1 and cavin-1 in the current experimental conditions. There may be additional layers of complexity involved in the interactions between the two proteins *in vivo.*

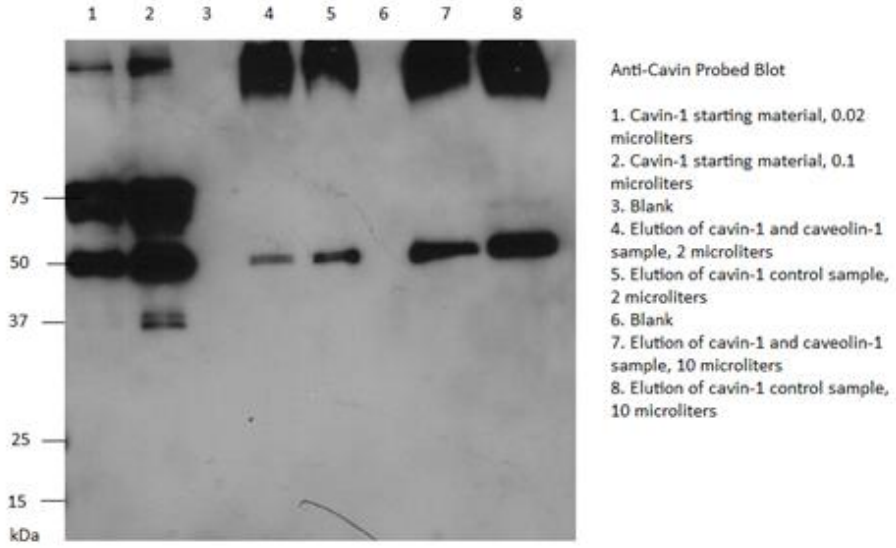

Figure 18b: Test for Binding of Caveolin-1 and Cavin-1. Samples were prepared on washed Ni-NTA beads, and eluted as described in Methods and Materials, section 2.5. The imidazole-eluted fractions were collected for SDS-PAGE and transferred to a PVDF membrane. The blot was probed with polyclonal rabbit anti-PTRF.

Chapter 4

DISCUSSION

In this study, I attempted to purify full-length cavin-1 for future use in binding experiments with caveolin-1 to learn about the mechanism of binding between the two coat proteins. Previous work in the lab had shown the GST-cavin-1 fusion construct was expressed moderately well and was partially soluble. When a 6xHis-SUMO fusion with a truncated cavin-3 construct (lab number: DB1480) was tested, there was much higher expression of that construct than other tagged versions of the same protein that were previously examined in the lab. For this reason, my initial studies began with making a 6x-His-SUMO-tagged full length-cavin-1 fusion, for comparison with our existing GSTS-cavin-1. I generated a plasmid encoding 6His-SUMO-cavin-1 by cloning *E. coli*-optimized full length cavin-1 into the LIC SUMO 2S-T vector, which contained the 6His-SUMO fusion tag. Earlier tests on 6His-SUMO-truncated-cavin-3 had shown that the LIC vector was leaky, leading to background expression of truncated cavin-3 even before IPTG-induction. However, using the BL21(DE3) pLysS strain reduced basal expression of heterologous cavin-3. To increase transformation efficiency, I modified the LIC SUMO vector using site-directed mutagenesis to change the SspI site to an SpeI site, in the hopes of having good ligation to transform BL21(DE3) pLysS cells. Sequencing results showed that the SUMO fusion with the full-length codon-optimized cavin-1 insert was successfully made.

The 6His-SUMO-cavin-1 construct (lab number: DB1493) was tested in small-scale trials to evaluate expression and solubility of the fusion protein before scaling up for purification. Soluble recombinant protein is necessary for studies of protein structure and function. (Gopal and Kumar, 2013). Parameters such as IPTG concentration, as well as temperature and length of incubation after IPTG induction were tested to determine if cavin-1 was expressed, and to determine the optimal conditions for future high-yield purifications. The 6His-SUMO-cavin-1 construct expressed a protein of the predicted ~75 kDa mass. Expression was highest after induction with 0.5 mM IPTG, and between 3-4 hours of incubation at 37˚C after IPTG induction. Despite successful expression, cavin-1 did not show consistent solubility during trials. Previous

work in the lab had shown that cavins are fairly insoluble after cell lysis, even when expressed in mammalian cells. The detergent, Fos choline-16, was compared to the routinely used detergent, Triton X-100, in its ability to solubilize recombinant cavin-1. The use of detergents can be valuable in membrane protein solubilization, as they can mimic the natural lipid bilayer environment of the native protein *in vivo* and can help proteins remain correctly folded in solution. Though cavin-1 is not an integral membrane protein, detergents, especially Fos choline 16, were found to greatly increase cavin solubility in mammalian cells in previous lab experiments. Neither detergent showed reliable solubilization of 6His-SUMO-cavin-1 from bacterial cell lysates (Figure 3) in the current study. However, when the duplicate Fos choline-16 treated samples were re-run on the gel (lanes 11 and 12 in Figure 3), the samples showed a higher fraction of soluble protein compared to insoluble protein, in contrast to the results in lanes 7 and 8 of Figure 3. Because soluble cavin-1 was detected (albeit in only one instance), Fos choline-16 was used in subsequent trials.

I performed IMAC tests to bind the 6His-tag to the Ni-NTA beads and assess release of 6His-SUMO-cavin-1 after eluting the protein from the beads with elution buffers containing 250 mM imidazole. The protein was successfully released during the two 250 mM imidazole elutions in the first IMAC test, but consistent elution was not obtained in further trials. I then tested the effects of adding Fos choline-16 at two different concentrations and elution with 0.1% N-lauroyl sarcosine on cavin-1 release. However, these approaches did not enhance protein release from Ni-NTA. Inefficient binding to the resin was a persistent issue as well. As a significant amount of the protein could not bind to the beads, yields of eluted protein were low. Taken together, tests on the 6His-SUMO-cavin-1 construct revealed problems with solubility, binding, and release of the protein, hindering cavin-1 purification efforts.

When heterologous genes, such as cavin-1, are expressed in foreign hosts, the desired protein can accumulate in the cytoplasm, rendering it difficult to obtain sufficient amounts of functional and stable protein from the native environment (Seddon et al., 2004). While cavins can interact with the plasma membrane, it is not known whether this is due to interactions with other peptidic components of the PM or possible interactions with the hydrophobic part of the

lipid bilayer. If the latter is true, cavins might have some hydrophobic character, making them prone to aggregation. The potential oligomerization of cavin-1 in the bacterial host may have led to complexes which bind the beads with high avidity, due to the increased number of physical and spatial interaction surface area. If high avidity binding explained poor elution with 250 mM imidazole, then the chelating agent, EDTA (which completely removes the nickel along with any complexed 6His protein- from the beads), would be expected to completely elute the protein. However, an EDTA elution did not show release of the protein, disproving the hypothesis that inefficient bead elution was due to high-avidity binding of a cavin-1 oligomer, and suggesting that cavin-1 was binding to the beads non-specifically.

Because of the poor results with the 6His-SUMO-cavin-1 construct, studies on the GST-cavin-1 construct expressed in BL21(DE3) were resumed. GST-cavin-1 was tested for binding to and release from glutathione-agarose beads. The effects of temperature and length of incubation after IPTG induction, detergent type and bead concentration on solubility and purified protein yield were investigated. Overall, results from these trials showed consistent, reliable recovery of purified cavin-1, and low but adequate release from beads after eluting the protein with a buffer composed of reduced glutathione, Tris and N-lauroyl sarcosine. Variations in temperature (29˚C and 37˚C) and length of incubation after IPTG induction (2-4 hours) did not dramatically affect GST-cavin-1 yields, as acceptable levels of expression were obtained in all tested conditions. However, the maximum potential yield of purified GST-cavin-1 was decreased due to lack of complete protein solubilization and persistent weak binding to the glutathione-agarose beads. The high quantity of unbound protein observed in each GST-cavin-1 test was typical of previous efforts with the construct, prompting the initial studies on 6His-SUMO-cavin-1. I tried increasing the bead concentration by a factor of 3 to maximize the probability of binding, but the quantity of unbound protein still exceeded the amount of protein in the eluted fraction. Incubating the BL21(DE3) culture at 16˚C after induction, to address potential protein mis-folding problems, did not resolve the binding problem. I was also unable to salvage residual GST-cavin-1 from the unbound protein fraction.

The problems observed with the GST-cavin-1 construct were not unique to this fusion, as similar issues arose with 6His-SUMO-cavin-1. The GST-cavin-1 may have folded into an unfavorable conformation or orientation that is not conducive to bead binding. The potential aggregation of cavin-1 may also be a potential explanation for the solubility and binding issues. Despite continual issues of solubility, and suboptimal binding, the GST-cavin-1 construct was successfully eluted from the glutathione-agarose beads, with a consistency not observed in 6His-SUMO-cavin-1 trials. The inadequate bead-binding problem may be overshadowed by the adequate release of protein in eluted fractions. While the quantity of the purified protein may not be high, its integrity might be retained. For studies of structure and function, it is important to obtain high quality protein that has retained integrity.

For the aforementioned reasons, GST-cavin-1 was selected as the construct of choice for large-scale protein purification. I performed a 2 liter preparation of GST-cavin-1 and was successfully able to obtain 30-60 μg of protein in 1.5 ml of eluate (with a concentration of ~30 μg/ml). This protein was used to perform a preliminary binding test with the previously obtained, IMAC-purified 6His-caveolin-1, on Ni-NTA beads (for anchoring the 6His-tag). Unfortunately, no binding between caveolin-1 and cavin-1 was observed.

The lack of binding between the coat proteins may be attributed to various factors that will need to be studied in future experiments. The stoichiometry of caveolin-1 and cavin-1 complexes is not well-characterized, and it is possible that the amounts used in this diagnostic test are insufficient for a high probability of binding interactions. The volumes of both cavin-1 and caveolin-1 need to be tested to determine the ideal ratio for increasing the probability of obtaining enough of each coat protein with the correct orientations for binding. In this experiment, the cavin-1/caveolin-1 sample was incubated for 2 hours at room temperature. However, the ideal temperature and duration of incubation with Ni-NTA is not known. It is possible that a higher incubation temperature will increase the frequency of collision between the two proteins, resulting in binding. The interactions between caveolin-1 and cavin-1 may be transient, so collection of samples at various time points may determine the ideal incubation length that will preserve association. It is also possible that both proteins are not in their native,

in vivo conformation, hindering favorable overlap between amino acid residues. The effect of N-lauroyl sarcosine (in the eluted fraction containing caveolin-1/cavin-1) on binding interactions, if any, remains unknown. The detergent may stabilize the proteins in solution and mimic the natural lipid environment. Conversely, N-lauroyl sarcosine may also block key sites of binding between the proteins. An elution without N-lauroyl sarcosine will need to be done to understand the effects of this detergent.

The lack of observed binding can be due to additional layers of complexity, inherent to the localization of cavin-1 and caveolin-1 *in vivo*. Cavin-1 only associates with caveolin-1 at the plasma membrane, and does not interact with Golgi-localized caveolin-1. This specificity contributes to the ability of cavin-1 to modulate the ratio of caveolar and non-caveolar caveolins (Chadda and Mayor, 2008). However, the molecular details of this exclusivity are not known. If the biochemical, functional and structural bases of this regulation can be determined, they may aid binding of the two coat proteins in this experiment. A combinatorial model for binding of cavin-1 to caveolin-1 is also likely. According to Kovtun and colleagues (2014), cavins may be anchored to the PM through the interactions of their basic HR1 domains and membrane phosphoinositides (Kovtun et al., 2014). Cholesterol availability also regulates binding between caveolin-1 and cavin-1. The depletion of cholesterol causes their dissociation (Parton and del Pozo, 2013). Since the samples in this preliminary experiment were not supplemented with phosphoinositides and cholesterol, the caveolin-1 and cavin-1 may not have had the necessary components for combinatorial binding and co-localization.

Further cavin-1 purification attempts will be required to optimize the yield of the protein for binding studies. For the 6His-SUMO-cavin-1, the experimental conditions in the expression/solubility and IMAC tests will need to be repeated to confirm the observed results. The orientation of the SUMO-tag can be changed from an N-terminal to C-terminal fusion to determine if cavin-1 solubility is improved and if 6His-binding to the nickel column is enhanced. For both GST-cavin-1 and 6His-SUMO-cavin-1 expressed in E. coli, the cavin-1 may have been packaged in inclusion bodies. Tao and colleagues (2010) were able to improve binding efficiency of GST fusions to Sepharose and recover soluble fusion proteins from inclusion bodies by using

a combination of three detergents, N-lauroyl sarcosine, Triton X-100 and CHAPS (Tao et al., 2010). This detergent combination can be tested in future experiments. It is possible that the detergents might hinder bead binding as well, so effects of their omission from wash and elution buffers should also be investigated. In future studies of binding between caveolin-1 and cavin-1, dialysis of the imidazole-eluted caveolin-1/cavin-1 sample containing Sarkosyl can be done to remove the detergent and for additional purification. Detergents can also lead to destabilization and inactivation of proteins over time, so alternative solubilizing agents, such as amphipol copolymers, can be tested to stabilize protein complexes (Seddon et al., 2004). Maintaining the stability of protein complexes will be crucial when testing binding of cavin-1 to liposome-incorporated caveolin-1, as described below, to avoid liposome solubilization by detergents used to maintain solubility of cavin-1. Cleaving the GST-fusion tag from GST-cavin-1 can be another approach to increasing the binding surface area with caveolin-1. An ideal system for *in vitro* membrane protein binding studies will strive to simulate the natural lipid bilayer that surrounds the proteins (Seddon et al., 2004). Reconstituting caveolin-1 and cavin-1 into phospholipid vesicles, proteoliposomes, can be a viable model for study. The addition of cholesterol and PIP2 to these proteoliposomes will mimic the in vivo environment of caveolae, and may facilitate combinatorial binding of the coat proteins. If binding tests between caveolin-1 and cavin-1 prove to be successful, further binding studies can be developed to define the interaction more precisely. Mutant versions of each coat protein can be generated to analyze the sequences responsible for interaction. These future explorations will help refine methods for the expression, co-purification and analysis of these caveolar coat proteins, as well as hone biotechniques for other membrane protein studies. Studies of cavin-1 and caveolin-1 interactions will strengthen our understanding of caveolae assembly and will provide valuable insight into the morphology of the mammalian plasma membrane.

References

1. Arnau, J., Lauritzen, C., Petersen, G. E., & Pedersen, J. (2006). Current strategies for the use of affinity tags and tag removal for the purification of recombinant proteins. *Protein expression and purification*, *48*(1), 1-13.
2. Bastiani, M., Liu, L., Hill, M. M., Jedrychowski, M. P., Nixon, S. J., Lo, H. P., ... & Parton, R. G. (2009). MURC/Cavin-4 and cavin family members form tissue-specific caveolar complexes. *The Journal of cell biology*, *185*(7), 1259-1273.
3. Brodsky, F. M., Chen, C. Y., Knuehl, C., Towler, M. C., & Wakeham, D. E. (2001). Biological basket weaving: formation and function of clathrin-coated vesicles. *Annual review of cell and developmental biology*, *17*(1), 517-568.
4. Brown DA and London E (1998) Functions of lipid rafts in biological membranes. *Annu Rev Cell Dev Biol.* **14**:111-136
5. Burgener, R., Wolf, M., Ganz, T., & Baggiolini, M. (1990). Purification and characterization of a major phosphatidylserine-binding phosphoprotein from human platelets. *Biochem. J*, *269*, 729-734.
6. Butt, T. R., Edavettal, S. C., Hall, J. P., & Mattern, M. R. (2005). SUMO fusion technology for difficult-to-express proteins. *Protein expression and purification*,*43*(1), 1-9.
7. Chadda, R., & Mayor, S. (2008). PTRF triggers a cave in. *Cell*, *132*(1), 23-24.
8. Chelur, D., Unal, O., Scholtyssek, M., & Strickler, J. (2008). Fusion tags for protein expression and purification.
9. Esposito, D., & Chatterjee, D. K. (2006). Enhancement of soluble protein expression through the use of fusion tags. *Current opinion in biotechnology*,*17*(4), 353-358.
10. Fra, A. M., Williamson, E., Simons, K., & Parton, R. G. (1994). Detergent-insoluble glycolipid microdomains in lymphocytes in the absence of caveolae. Journal of Biological Chemistry, 269(49), 30745-30748.
11. Fuguet, E., Ràfols, C., Rosés, M., & Bosch, E. (2005). Critical micelle concentration of surfactants in aqueous buffered and unbuffered systems.*Analytica Chimica Acta*, *548*(1), 95-100.
12. Gabella, G. (1976). Quantitative morphological study of smooth muscle cells of the guinea-pig taenia coli. Cell and tissue research, 170(2), 161-186.
13. Gambin, Y., Ariotti, N., McMahon, K. A., Bastiani, M., Sierecki, E., Kovtun, O., ... & Parton, R. G. (2014). Single-molecule analysis reveals self assembly and nanoscale segregation of two distinct cavin subcomplexes on caveolae. *Elife*, *3*, e01434.
14. Gil, J. (1983, May). Number and distribution of plasmalemmal vesicles in the lung. In Federation proceedings (Vol. 42, No. 8, pp. 2414-2418).

15. Glenney, J. R., & Zokas, L. (1989). Novel tyrosine kinase substrates from Rous sarcoma virus-transformed cells are present in the membrane skeleton. *The Journal of Cell Biology*, *108*(6), 2401-2408.
16. Gopal, G. J., & Kumar, A. (2013). Strategies for the production of recombinant protein in Escherichia coli. *The protein journal*, *32*(6), 419-425.
17. Hammarström, M., Hellgren, N., van den Berg, S., Berglund, H., & Härd, T. (2002). Rapid screening for improved solubility of small human proteins produced as fusion proteins in Escherichia coli. *Protein Science*, *11*(2), 313-321.
18. Hansen, C. G., & Nichols, B. J. (2010). Exploring the caves: cavins, caveolins and caveolae. *Trends in cell biology*, *20*(4), 177-186.
19. Harper, S., & Speicher, D. W. (2011). Purification of proteins fused to glutathione S-transferase. In *Protein Chromatography* (pp. 259-280). Humana Press.
20. Hill, M. M., Bastiani, M., Luetterforst, R., Kirkham, M., Kirkham, A., Nixon, S. J., ... & Parton, R. G. (2008). PTRF-Cavin, a conserved cytoplasmic protein required for caveola formation and function. *Cell*, *132*(1), 113-124.
21. IBA-Life Sciences (2012). *Expression and purification of proteins using 6xHistidine-tag: A comprehensive manual.* Goettingen, Germany.
22. Jansa, P., Mason, S. W., Hoffmann-Rohrer, U., & Grummt, I. (1998). Cloning and functional characterization of PTRF, a novel protein which induces dissociation of paused ternary transcription complexes. *The EMBO Journal*,*17*(10), 2855-2864.
23. Kovtun, O., Tillu, V. A., Jung, W., Leneva, N., Ariotti, N., Chaudhary, N., ... & Collins, B. M. (2014). Structural insights into the organization of the cavin membrane coat complex. *Developmental cell*, *31*(4), 405-419.
24. Krijnse Locker, J., & Schmid, S. L. (2013). Integrated electron microscopy: super-duper resolution. *PLoS Biol*, *11*(8), e1001639.
25. Kurzchalia, T. V., Dupree, P., Parton, R. G., Kellner, R., Virta, H., Lehnert, M., & Simons, K. (1992). VIP21, a 21-kD membrane protein is an integral component of trans-Golgi-network-derived transport vesicles. The Journal of cell biology, 118(5), 1003-1014.
26. Le Lay, S., & Kurzchalia, T. V. (2005). Getting rid of caveolins: phenotypes of caveolin-deficient animals. Biochimica et Biophysica Acta (BBA)-Molecular Cell Research, 1746(3), 322-333.
27. Life Technologies (2010). *Champion™ pET SUMO Protein Expression System User Manual.* Carlsbad, California.
28. Lisanti, M. P., Scherer, P. E., Vidugiriene, J., Tang, Z., Hermanowski-Vosatka, A., Tu, Y. H., ... & Sargiacomo, M. (1994). Characterization of caveolin-rich membrane domains isolated from an endothelial-rich source: implications for human disease. *The Journal of cell biology*, *126*(1), 111-126.

29. Ludwig, A., Howard, G., Mendoza-Topaz, C., Deerinck, T., Mackey, M., Sandin, S., ... & Nichols, B. J. (2013). Molecular composition and ultrastructure of the caveolar coat complex.
30. Malakhov, M. P., Mattern, M. R., Malakhova, O. A., Drinker, M., Weeks, S. D., & Butt, T. R. (2004). SUMO fusions and SUMO-specific protease for efficient expression and purification of proteins. *Journal of structural and functional genomics*, *5*(1-2), 75-86.
31. Mobley, B. A., & Eisenberg, B. R. (1975). Sizes of components in frog skeletal muscle measured by methods of stereology. *The Journal of general physiology*,*66*(1), 31-45.
32. Mogelsvang, S., Marsh, B. J., Ladinsky, M. S., & Howell, K. E. (2004). Predicting function from structure: 3D structure studies of the mammalian Golgi complex. *Traffic*, *5*(5), 338-345.
33. Monier, S., Parton, R. G., Vogel, F., Behlke, J., Henske, A., & Kurzchalia, T. V. (1995). VIP21-caveolin, a membrane protein constituent of the caveolar coat, oligomerizes in vivo and in vitro. Molecular Biology of the Cell, 6(7), 911-927.
34. Napolitano, L. (1963). The differentiation of white adipose cells an electron microscope study. *The Journal of cell biology*, *18*(3), 663-679.
35. Nilsson, J., Ståhl, S., Lundeberg, J., Uhlén, M., & Nygren, P. Å. (1997). Affinity fusion strategies for detection, purification, and immobilization of recombinant proteins. *Protein expression and purification*, *11*(1), 1-16.
36. Park, D. S., Woodman, S. E., Schubert, W., Cohen, A. W., Frank, P. G., Chandra, M., ... & Lisanti, M. P. (2002). Caveolin-1/3 double-knockout mice are viable, but lack both muscle and non-muscle caveolae, and develop a severe cardiomyopathic phenotype. The American journal of pathology, 160(6), 2207-2217.
37. Parton, R. G., & del Pozo, M. A. (2013). Caveolae as plasma membrane sensors, protectors and organizers. *Nature reviews Molecular cell biology*,*14*(2), 98-112.
38. Pelkmans, L., & Zerial, M. (2005). Kinase-regulated quantal assemblies and kiss-and-run recycling of caveolae. Nature, 436(7047), 128-133.
39. Predescu, D., Horvat, R., Predescu, S., & Palade, G. E. (1994). Transcytosis in the continuous endothelium of the myocardial microvasculature is inhibited by N-ethylmaleimide. *Proceedings of the National Academy of Sciences*, *91*(8), 3014-3018.
40. Razani, B., Woodman, S. E., & Lisanti, M. P. (2002). Caveolae: from cell biology to animal physiology. *Pharmacological reviews*, *54*(3), 431-467.
41. Rothberg KG, Heuser JE, Donzell WC, Ying YS, Glenney JR, and Anderson RG (1992) Caveolin, a protein component of caveolae membrane coats. *Cell* **68:**673-682.
42. Seddon, A. M., Curnow, P., & Booth, P. J. (2004). Membrane proteins, lipids and detergents: not just a soap opera. *Biochimica et Biophysica Acta (BBA)-Biomembranes*, *1666*(1), 105-117.
43. Simons, K., & Toomre, D. (2000). Lipid rafts and signal transduction. *Nature reviews Molecular cell biology*, *1*(1), 31-39.

44. Sowa, G. (2011). Novel insights into the role of caveolin-2 in cell-and tissue-specific signaling and function. *Biochemistry research international*, *2011*.
45. Tao, H., Liu, W., Simmons, B. N., Harris, H. K., Cox, T. C., & Massiah, M. A. (2010). Purifying natively folded proteins from inclusion bodies using sarkosyl, Triton X-100, and CHAPS. *Biotechniques*, *48*(1), 61-64.
46. Tagawa, A., Mezzacasa, A., Hayer, A., Longatti, A., Pelkmans, L., & Helenius, A. (2005). Assembly and trafficking of caveolar domains in the cell caveolae as stable, cargo-triggered, vesicular transporters. The Journal of cell biology, 170(5), 769-779.
47. Vereb, G., Szöllősi, J., Matko, J., Nagy, P., Farkas, T., Vigh, L. M. L. W. T. A., ... & Damjanovich, S. (2003). Dynamic, yet structured: the cell membrane three decades after the Singer–Nicolson model. *Proceedings of the National Academy of Sciences*, *100*(14), 8053-8058.
48. Vinten, J., Johnsen, A. H., Roepstorff, P., Harpøth, J., & Tranum-Jensen, J. (2005). Identification of a major protein on the cytosolic face of caveolae.*Biochimica et Biophysica Acta (BBA)-Biomembranes*, *1717*(1), 34-40.